anatomia

MDPI

Article

Histological Characterization of Ocular and Adnexal Tissues in Dogs (*Canis familiaris*) and Wolves (*Canis lupus*)

Abel Diz López [1,†], Mateo V. Torres [2,†], Fabio Martínez Gómez [3], Silvia Alejandra Fraga Abelleira [4], Ana López-Beceiro [4], Luis Fidalgo [4], Pablo Sanchez-Quinteiro [4,*] and Irene Ortiz-Leal [4]

1 Anicura Navia Hospital Veterinario, 36212 Vigo, Spain; abel.diz.lopez@gmail.com
2 Research Center for Molecular Medicine and Chronic Diseases (CIMUS), Instituto de Investigación Sanitaria (IDIS), University of Santiago de Compostela, 15705 Santiago de Compostela, Spain; mateovazquez.torres@usc.es
3 Willows Veterinary Centre and Referral Service, Solihull B90 4NH, UK; fabio.mg@telefonica.net
4 Department of Anatomy, Animal Production and Clinical Veterinary Sciences, Faculty of Veterinary, University of Santiago de Compostela, 27002 Lugo, Spain; silviaalejandra.fraga@rai.usc.es (S.A.F.A.); anam.lopez.beceiro@usc.es (A.L.-B.); luis.fidalgo@usc.es (L.F.); irene.ortiz.leal@usc.es (I.O.-L.)
* Correspondence: pablo.sanchez@usc.es
† These authors contributed equally to this work.

Abstract

Background/Objectives: This study explores the ocular anatomy and glandular components of domestic dogs compared to their ancestor, the wolf, with the aim of identifying evolutionary changes due to domestication and their implications for ocular pathologies. Methods: Utilizing histological and histochemical techniques, including hematoxylin–eosin, Periodic Acid–Schiff, Alcian Blue, and lectins, this research conducts a detailed analysis of the canine and wolf ocular systems, focusing on the eyelids, tarsal glands, and conjunctival tissues. Results: There are marked histological differences between the two species, particularly in the thickness and secretion levels of the conjunctival epithelia and the structure of the tarsal glands. Dogs exhibit a thicker epithelium with greater Periodic Acid–Schiff and Alcian Blue positive secretion, suggesting enhanced ocular protection and lubrication adapted to domestic environments. Conversely, wolves display more concentrated glandular secretions and a predominance of acidic mucopolysaccharides, aligning with their adaptation to natural habitats. Conclusions: Although this study is constrained by the limited number of samples, the use of mixed dog breeds, and the focus on the Iberian wolf, it nonetheless suggests histological and evolutionary differences between domestic dogs and wolves, particularly in structures related to ocular surface protection and lubrication. These differences likely reflect adaptive responses to domestication in dogs and environmental demands in wolves. Importantly, the findings emphasize the clinical and translational potential of using dogs as comparative models for human ocular surface disorders, given their anatomical proximity to humans.

Keywords: ocular system; ocular adnexa; dog; wolf; tarsal glands; mucous glands; lectins; glycoconjugates

Academic Editor: Francesco Fornai

Received: 16 April 2025
Revised: 21 June 2025
Accepted: 23 June 2025
Published: 25 June 2025

Citation: Diz López, A.; Torres, M.V.; Martínez Gómez, F.; Fraga Abelleira, S.A.; López-Beceiro, A.; Fidalgo, L.; Sanchez-Quinteiro, P.; Ortiz-Leal, I. Histological Characterization of Ocular and Adnexal Tissues in Dogs (*Canis familiaris*) and Wolves (*Canis lupus*). *Anatomia* **2025**, *4*, 10. https://doi.org/10.3390/anatomia4030010

1. Introduction

The eyelids, including the lower, upper, and third eyelids; bulbar and palpebral conjunctiva; and lacrimal apparatus and their associated glands, are not involved in vision, but play a fundamental role in ocular protection in animals [1]. Similarly, the ocular surface,

formed by the corneal, limbal, and conjunctival epithelia, along with the tear film, plays a vital role in protecting the eye [2]. The hermetic barrier formed by the corneal epithelium is necessary for preventing the entrance of pathogens. The weak point of this barrier is its transparency and lack of blood vessels for nutrition; however, this disadvantage is compensated for by the support provided by the limbal tissue [3]. The limbal tissue, as its name suggests, is a transition to the conjunctiva, a highly vascularized mucosal tissue that provides excellent protection against infections and antigens [4]. The mucin-secreting goblet cells in the conjunctiva perform a crucial protective function. These mucins, along with secretions from the lacrimal and tarsal glands, also known as Meibomian glands, form the tear film [5]. Alterations in goblet cell function change tear composition, leading to various pathologies. Additionally, conjunctiva-associated lymphoid tissue (CALT), which consists of B and T lymphocytes, macrophages, and dendritic cells, initiates and regulates immune responses [6,7].

Since ancient times, dogs have been recognized for their close relationship with humans, a continuing historical coexistence [8]. This relationship has brought many advantages to both species. However, domestication and the intense artificial selection imposed by humans [9] may be responsible for various pathologies in dogs, including ocular problems such as conjunctivitis, dry keratoconjunctivitis [10], and other inflammatory and dryness-related conditions. Inflammatory diseases such as keratoconjunctivitis sicca (KCS) result from abnormalities in the tear film, specifically in the glandular component, highlighting the significance of this component and its evolution [11].

Directly comparing the dog ocular system with that of their ancestor, the wolf, could reveal insights into the evolution of this system in dogs. This study aimed to characterize the eyeballs of domestic dogs and wolves, focusing on their glandular components, and to compare them to identify possible differences that support the hypothesis of artificial evolution due to domestication. To the best of our knowledge, the glandular component of the wolf eyeball has not been previously described. Furthermore, the only existing comparison of dog and wild canids' eyeballs focused on the dog and the crab-eating fox [12], and only routine histological stains were performed. However, recent anatomical and functional studies have revealed that wolves exhibit distinct ocular adaptations, such as high rod density, a well-developed tapetum lucidum, and a prominent visual streak and area centralis, all of which support optimized vision under low-light and complex environmental conditions [13]. These findings underscore the relevance of wolf ocular anatomy beyond evolutionary interest, providing crucial reference data for species-specific visual ecology. Moreover, although clinical ophthalmologic data in wolves are scarce, isolated case reports have documented disorders such as KCS and chronic superficial keratitis [14,15], reinforcing the potential diagnostic and translational value of this type of research in both clinical and conservation settings.

Additionally, studying the ocular system of canids holds significant translational value for human ophthalmology. Human tissues are difficult to study and obtain; thus, animal research is essential. Previous studies have been conducted in pigs [3], and this study will follow a similar approach in dogs. Preclinical animal studies play a crucial role in enhancing our understanding of human diseases and advancing medical knowledge. However, there are notable disadvantages to using traditional laboratory animals, such as rabbits, mice, and rats, as models for the human ocular surface. For example, in rabbits, the ratio of conjunctival to corneal surface area is approximately two-fold lower than that in humans, which may affect tear distribution and drug absorption [16]. In addition, anatomical and physiological differences can alter the volume, stability, and breakdown dynamics of tear fluid [17]. For example, rabbits have a thinner corneal epithelium than humans, demonstrating reduced blinking frequency and distinct tear film composition. Furthermore, unlike human cells,

rabbit corneal endothelial cells retain their proliferative capacity, and their immune and inflammatory responses differ, limiting the translational value of such models [18]. The integration of companion dogs into preclinical pharmacology studies addresses these limitations. Dogs, which share closer anatomical and physiological similarities with humans in terms of ophthalmology, are valuable models for investigating ocular surface disorders. By utilizing dogs as preclinical models, researchers can gain a deeper understanding of the pathophysiology of ocular diseases, evaluate potential therapeutic interventions, and ultimately develop more effective treatment strategies for human patients. This approach has accelerated the development and application of ophthalmic research, bridging the gap between preclinical studies and clinical practice [19–22].

This study investigated the eyelids, tarsal glands, palpebral conjunctiva, bulbar conjunctiva, fornix, cornea, ciliary body, and lacrimal gland in dogs and wolves. The sclera, choroid, and retina were also examined in a more complementary manner. For this characterization, macroscopic and microscopic analyses were conducted using histological and histochemical techniques, including hematoxylin–eosin, periodic acid–Schiff (PAS), Alcian Blue, and lectins. The PAS stains neutral polysaccharides and mucopolysaccharides red, while Alcian Blue stains acidic polysaccharides blue, allowing the differentiation of the two glandular components. Lectin staining, targeting agglutinin proteins, was used to reveal glycoconjugates. This technique detects glycogen in the glands; thus, it is critical for characterizing the glandular component [23].

2. Materials and Methods

2.1. Samples

The eyeballs and their adnexa used in this study were collected from three adult mesocephalic male mixed-breed dogs, *Canis lupus familiaris*, that were sourced from the Rof Codina University Veterinary Hospital at the Faculty of Veterinary Sciences of Lugo. These dogs had died from various clinical conditions. Although their exact breed ancestry was unknown, all three dogs exhibited similar external morphology and cranial proportions and were classified as mesocephalic based on veterinary examination. Additionally, eyeballs were obtained from three adult male *Canis lupus signatus* whose carcasses originated from wildlife rehabilitation centers in the provinces of Galicia and had died due to fatal accidents. All individuals included in the study were adult males in order to reduce biological variability related to sex. In the case of dogs, the eyes were collected within 2 to 3 h following euthanasia. For the wolves, which had died due to traffic accidents, the exact post-mortem interval could not be precisely determined; however, according to the records from the wildlife rehabilitation centers, it did not exceed 12 h in any case. None of the dogs included in the study presented clinical signs or had a prior diagnosis of ocular disease. This information was confirmed through available veterinary records and general clinical examination. In the case of the wolves, no ocular anomalies were observed during post-mortem inspection. The estimated age of all animals ranged between 5 and 10 years. Although exact body weights were not recorded, veterinary records and body condition suggested approximate weights of 20–30 kg for the dogs and 30–40 kg for the wolves. None of the samples were frozen at any point in order to prevent the formation of ice crystals that could compromise tissue integrity and the quality of microscopic analysis. All procedures involving wild animals were carried out under the authorization of the Galician Environment, Territory, and Housing Department, under the approval codes EB-009/2020 and EB-007/2021. Although the permit authorization also included foxes, no fox samples were used in this study. All anatomical regions of interest were examined in each individual, and the same histological and histochemical processing protocols were

applied across all specimens. No relevant intra-species variability was observed among the dog samples in the present study.

2.2. Sample Dissection and Processing

The sample extraction process involved making an oval incision around the eyelids, preserving them, as they contain most of the glandular components, and exposing the orbit. Once the conjunctiva was secured with forceps, it was dissected along the bony orbital rim, providing access to the orbital cavity. Through this opening, we introduced blunt curved scissors to detach the extraocular muscles and the optic nerve, ultimately extracting the eyeball along with all associated structures. Once extracted, the eyeballs were immediately immersed in Bouin's solution, which penetrates tissue more effectively than formalin, better preserves the tissue, and provides more firmness. After 24 h, the eyeballs were bisected along a sagittal plane passing through the anteroposterior axis of the eye. Then, they were transferred to 70% ethanol. The samples were embedded in paraffin and serially cut into 7-micron-thick sections using a rotating microtome. The sections were collected on gelatinized slides and stored in an oven at 50 °C.

2.3. General Histological Stains

For the realization of this study, we used the following stains:

Hematoxylin–eosin (H-E): Slides were stained with hematoxylin (Merck, Darmstadt, Germany) and eosin (Sigma-Aldrich, St. Louis, MO, USA) following standard protocols.

PAS: Stain of choice for the detection of neutral polysaccharides. It allows differentiation of glycogen-rich and glycogen-poor areas, as well as appreciation of mucous secretions from glandular components. In addition, it is also suitable for the visualization of cartilage and basal membranes [24]. The staining was carried out following the procedure described by Torres et al. [25]. The basis of the reaction consists of oxidizing the tissue with periodic acid (PanReac AppliChem, Barcelona, Spain) and subsequently applying Schiff's reagent (Merck, Germany), which reacts with aldehyde groups to produce a purple coloration in mucous glands.

Alcian Blue (AB): Alcian Blue staining was performed following the protocol described by Sanmartín-Vázquez et al. [26]. Alcian Blue (Sigma-Aldrich, St. Louis, MO, USA) binds to acidic mucopolysaccharides, producing a bluish coloration.

PAS-AB: Combined Alcian Blue–PAS staining was performed following the protocol described by Salazar et al. [27]. This technique allows simultaneous visualization of acidic mucopolysaccharides (stained blue by Alcian Blue) and neutral mucopolysaccharides (stained purple by PAS), providing a clear contrast in glandular tissues.

2.4. Lectin Histochemical Labelling

The histochemical staining procedures employed in this study involved techniques based on the specific binding of lectins. Lectins, primarily of plant origin, are a type of agglutinin that possesses domains capable of recognizing and binding to terminal carbohydrate residues in tissue glycoconjugates [28]. This interaction results in biotinylated complexes, which are then detected using an ABC complex with peroxidase. Unlike immunohistochemical techniques, lectins do not have an immune origin and are widely distributed in both animal and plant tissues, where they perform a variety of functions [29]. In this study, we employed two different lectins to characterize the glands present in the adnexa of the eyes.

LEA: Lectin corresponding to an agglutinin extracted from tomato (*Lycopersicum esculentum*) that has a high affinity for *N*-acetylglucosamine, which in turn binds to a specific carbohydrate [30].

UEA: Lectin corresponding to agglutinin from gorse (*Ulex europeaus*) that preferentially binds terminal L-fucose belonging to glycoproteins and glycolipids [31].

The rehydrated slides were initially subjected to a blocking step using 2% bovine serum albumin (BSA) to prevent nonspecific binding, followed by labeling with lectins. For UEA labeling, the samples were incubated for 1 h with unconjugated UEA lectin (L-1060; Vector Labs, Burlingame, CA, USA). Subsequently, a peroxidase-conjugated anti-UEA antibody (Dako, Glostrup, Denmark) was added, and the slides were incubated overnight. In the case of LEA labelling, a biotinylated lectin (B-1175-1; Vector Labs) was used and incubated overnight. The next day, the slides were incubated for one and a half hours with an ABC complex (Vectastain, Vector Labs) consisting of peroxidase and an avidin–biotin complex, which binds to the lectin. Visualization of the reaction was achieved using a solution of 0.003% hydrogen peroxide and 0.05% 3,3-diaminobenzidine (DAB) in a 0.2 M Tris–HCl buffer, producing a brown-colored deposit. The detailed procedure is explained in Ortiz-Leal et al. [32].

2.5. Imaging and Digital Processing

To obtain the digital images shown in this study, we used the following equipment and software:

Photomicroscope: An Axiophot microscope from Karl Zeiss (Jena, Germany)—ZEISS ZEN vs. 3.12—equipped with a digital camera, model MRc5 Axiocam, enabled high-resolution imaging of large sample areas. This is achieved by adjusting parameters such as white balance, exposure, focus, and shading prior to image acquisition.

Automatic fusion program: PTGui—version 12.27—(Rotterdam, The Netherlands): This software allowed us to merge the photographs obtained with the photomicroscope using common references points (control points) shared across the individual images, obtaining a final mosaic of excellent quality of the entire sample (in variable number from 6 to 300 photos, depending on the sample) resulting in the final digital image that we will use (Figure 1).

Adobe Photoshop CS4—version 21.2.4—(Adobe Systems, San Jose, CA, USA): We used this software for all the images where it was necessary to adjust contrast, brightness, and white balance digitally. No features were enhanced, added, or relocated in any of the images.

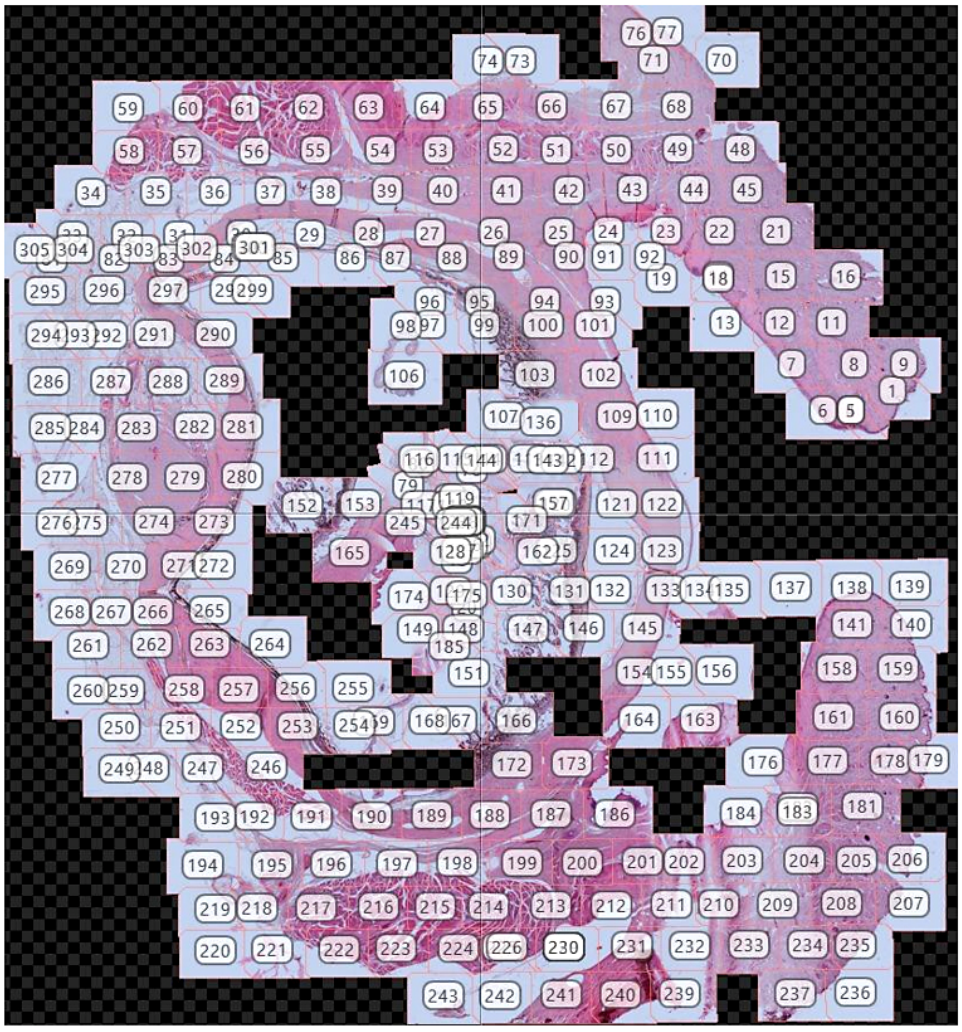

Figure 1. Composite mosaic constructed from 305 micrographs of a sagittal section of a wolf eye, with image numbering corresponding to the sequential order of acquisition.

3. Results

3.1. Macroscopic Study

As a preliminary step to the microscopic study, the eyeballs were extracted along with the eyelids and all other ocular adnexa structures contained within the orbit. The high penetrating power of Bouin's solution preserved the integrity of the structures within the eyeball without requiring dissection of the orbit. Only after fixation was the eyeball sectioned into two sagittal halves as illustrated in Figure 2. This image displays the principal anatomical components of the eyeball: the outer tunic, composed of the sclera and cornea; the middle tunic, consisting of the choroid, iris, and ciliary body; and the inner tunic formed by the blind and optic portions of the retina. Moreover, since this fixation method does not alter the shape of the eyeball, the three chambers—anterior, posterior, and vitreous—can be recognized. No macroscopic differences were observed between dogs and wolves. All elements accompanying the eyeball were preserved in these specimens. The protective structures around the optic nerve, particularly the Tenon's capsule (also known as the bulbar sheath), were notably difficult to section microtomically, although this did not prevent the completion of full histological sections of the eyeball as shown in the following section (Figure 3).

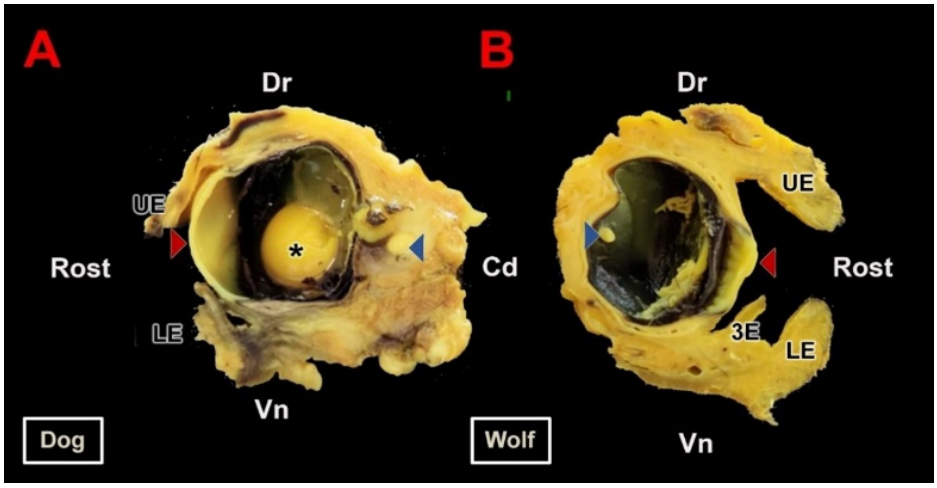

Figure 2. Macroscopic section of the canid eyeball. (**A**). Sagittal section of the right eyeball of the dog along its optic axis. (**B**). Sagittal section of the left eyeball of the wolf. Samples fixed in Bouin's fluid and postfixed in 70% ethanol. Cd, caudal; Dr, dorsal; LE, lower eyelid; UE, upper eyelid; Rost, rostral; Vn, ventral; 3E, third eyelid; *, lens; Red arrow, cornea; Blue arrow, retina.

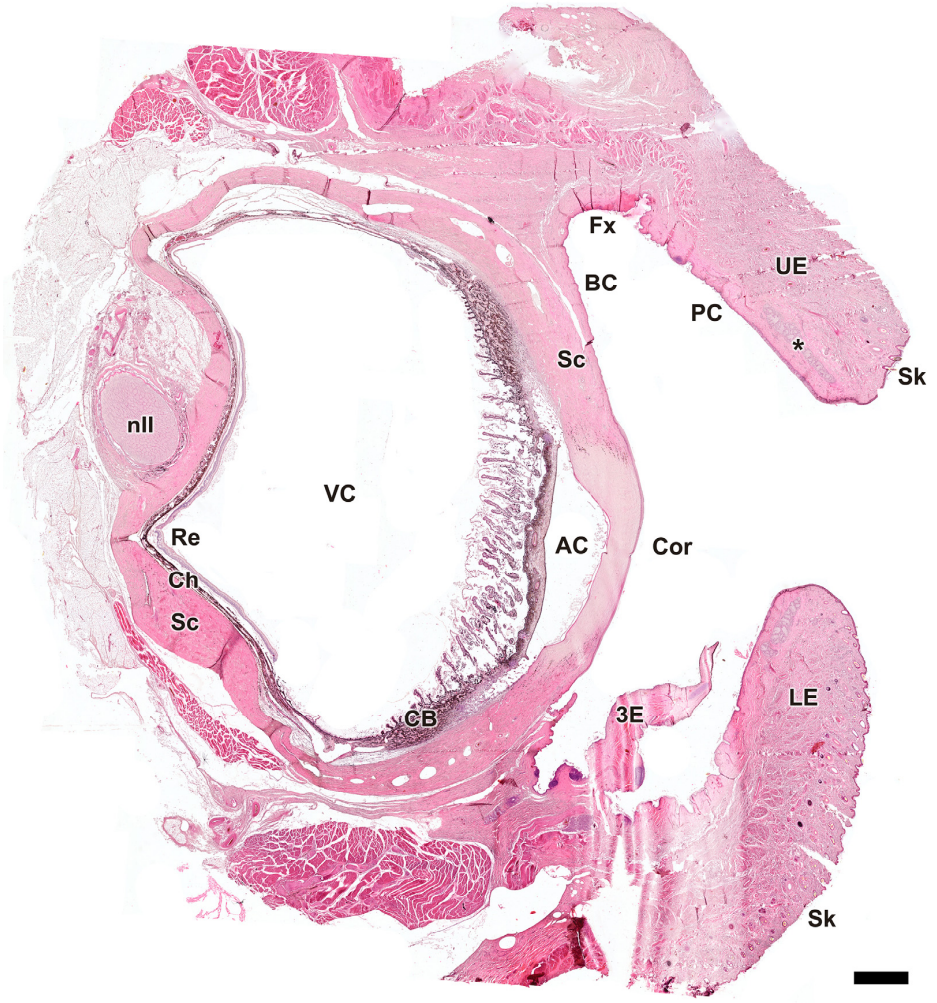

Figure 3. Microscopic sagittal section of the eye of *Canis lupus signatus*. AC, anterior chamber; BC, bulbar conjunctiva; CB, ciliary body; Ch, choroid; Cor, cornea; Fx, fornix; LE, lower eyelid; nII, optic nerve; PC, palpebral conjunctiva; Re, retina; Sc, sclera; Sk, skin; UE, upper eyelid; VC, vitreous chamber; 3E, third eyelid; *, tarsal glands. Hematoxylin–eosin staining. Scale bar = 500 µm.

3.2. Microscopic Study

As an initial step in the microscopic study, complete sagittal sections of the eyeball and associated adnexal structures were obtained from both wolf and dog specimens (Figures 3 and 4). Examination of these sections allowed identification of the regions involved in glandular secretion that were the subject of subsequent specific studies with hematoxylin–eosin, Alcian Blue, PAS, and PAS–Alcian Blue.

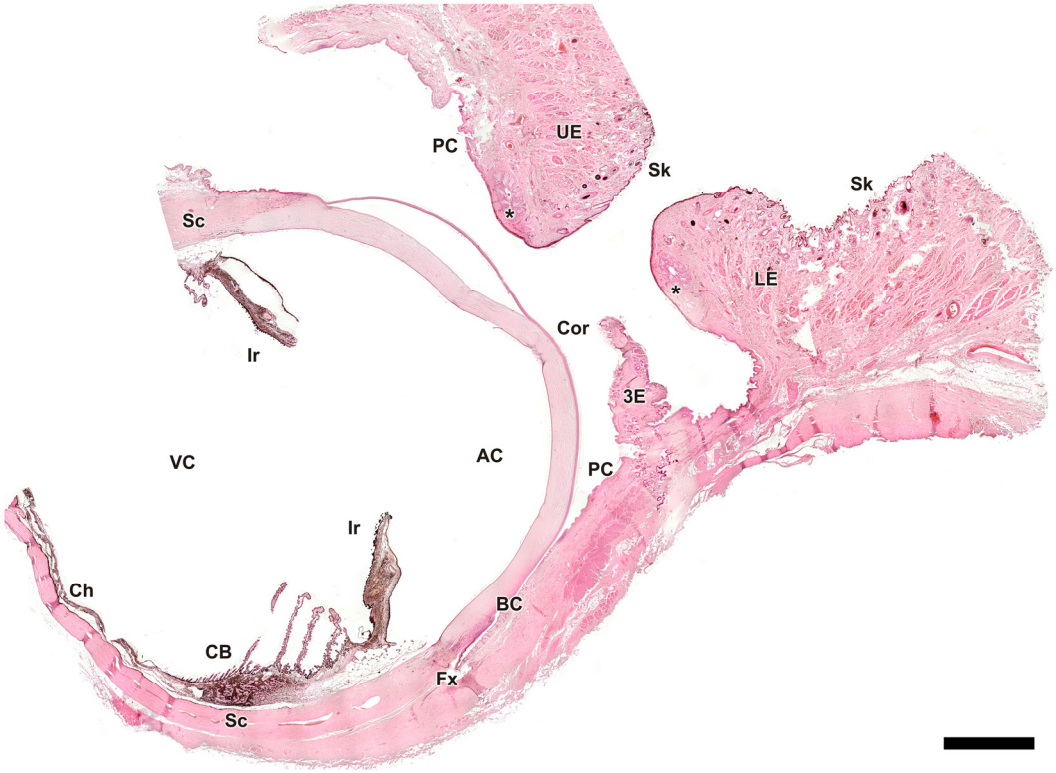

Figure 4. Microscopic sagittal section of the eye of *Canis familiaris*. AC, anterior chamber; BC, bulbar conjunctiva; CB, ciliary body; Ch, choroid; Cor, cornea; Fx, fornix; Ir, iris; LE, lower eyelid; PC, palpebral conjunctiva; Sc, sclera; Sk, skin; UE, upper eyelid; VC, vitreous chamber; 3E, third eyelid; *, tarsal glands. Hematoxylin-eosin staining. Scale bar = 500 µm.

3.2.1. Eyelid Skin Lining

Upon dissecting the eyeball, examination of the cutaneous lining of the palpebral region revealed a remarkable development of its dermal layer, which became more evident following staining with various histological stains, including hematoxylin–eosin, Alcian Blue, PAS, and PAS–Alcian Blue. As shown in Figure 5, comparative analysis indicates that both dogs and wolves exhibit similar histological characteristics, including non-keratinized stratified squamous epithelium, hair follicles, and connective tissue. Notably, glandular elements are abundant in the superficial dermis, with a higher prevalence noted in the dog (Figure 5C).

3.2.2. Upper Eyelid and Lower Eyelid

The histological examination of the eyelid revealed that both species display well-developed eyelid structures, including the epidermis, dermis, hair follicles, and palpebral conjunctiva (Figure 6). The glandular elements are mainly represented by the tarsal or Meibomian glands, along with the glands of Moll and the glands of Zeis. In both dogs (Figures 6–8) and wolves (Figures 7 and 8), there is abundant collagen, strongly PAS-positive.

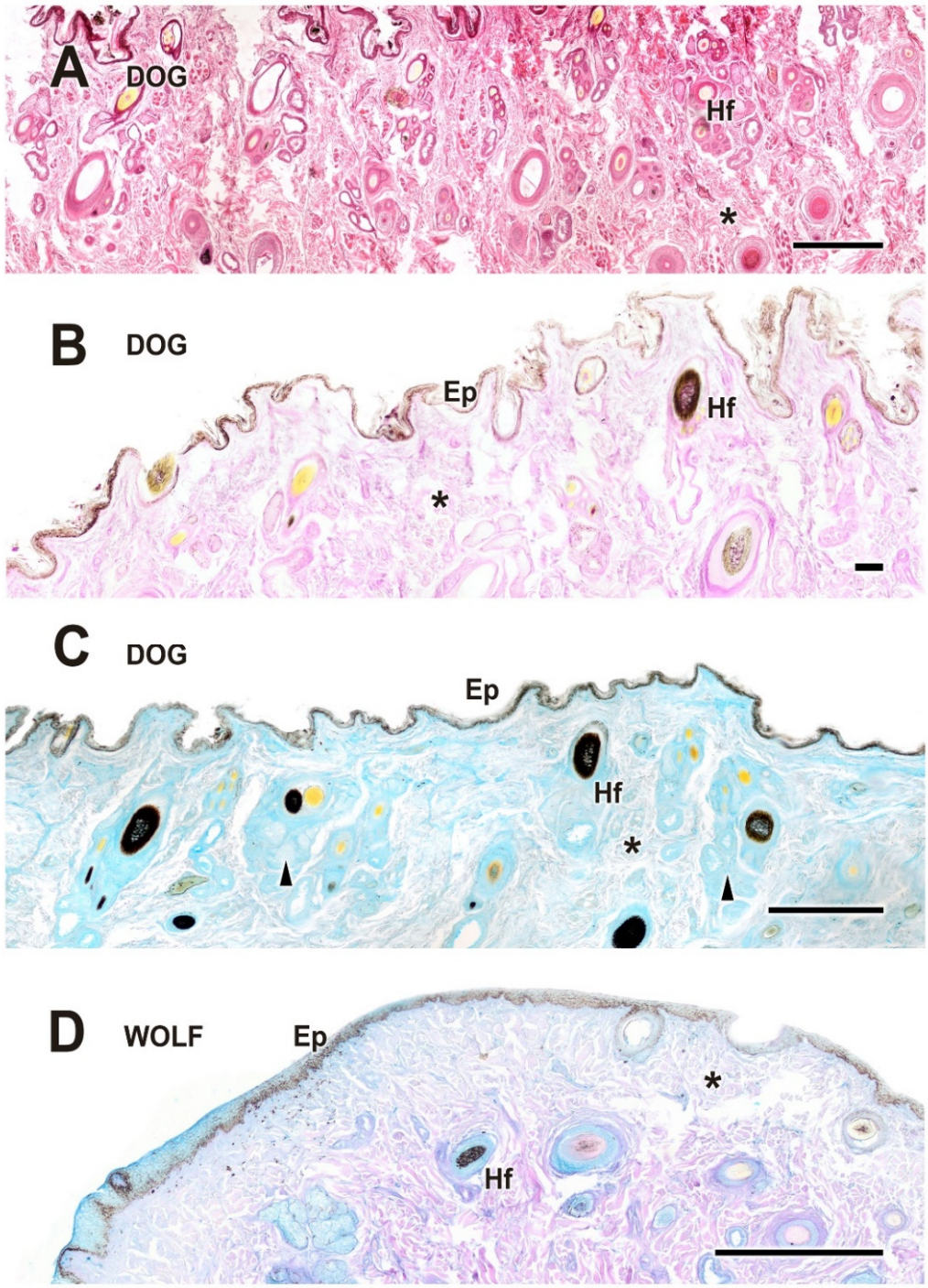

Figure 5. Histological study of the eyelid skin lining in the dog (**A**–**C**) and the wolf (**D**). The four histological stains used are hematoxylin–eosin (**A**), PAS (**B**), AB (**C**), and PAS-AB (**D**), which enable the characterization of the structure of the hair follicles, as well as the epidermis, dermis, and connective tissue development. Ep, epidermis; Hf, hair follicle; arrowheads, tubular glands; *, connective tissue. Scale bar: (**A**,**C**,**D**) = 500 μm; (**B**) = 100 μm.

This connective tissue is interspersed with numerous bundles of orbicularis oculi muscle fibers. In dogs, the connective tissue is more developed, which may account for the increased elasticity and relative ease of eyelid dissection compared to wolves, which exhibit a denser and more fibrous structure.

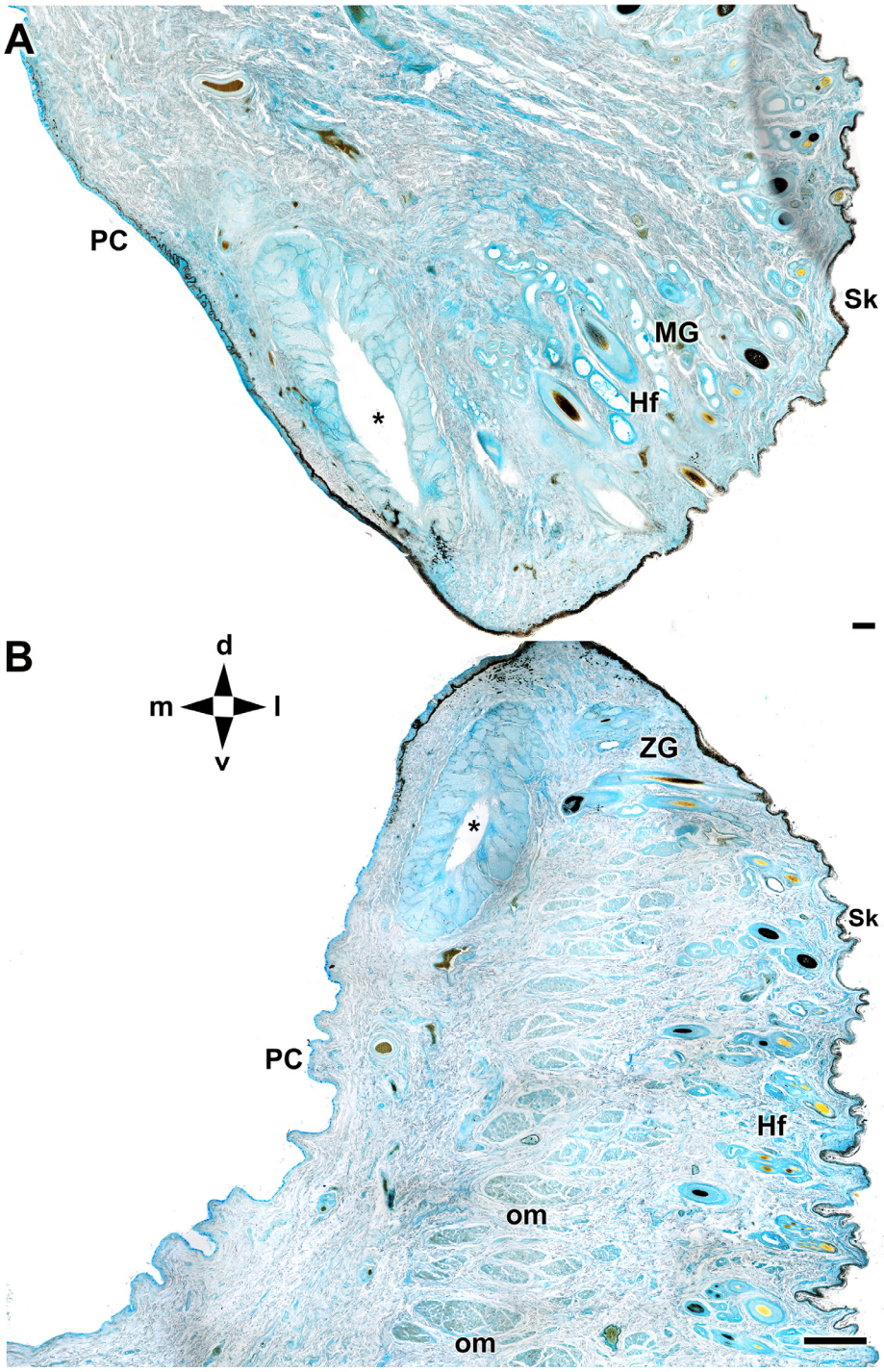

Figure 6. Microscopic anatomy of dog eyelids. The cross section allows identification of the main glandular elements of the upper (**A**) and lower (**B**) eyelid of the dog. d, dorsal; l, lateral; m, medial; PC, palpebral conjunctiva; Hf, hair follicle; MG, Moll's gland; om, orbicularis muscle; Sk, skin; v, ventral; ZG, Zeis gland; *, tarsal glands. AB staining. Scale bar: (**A**) = 100 µm; (**B**) = 500 µm.

3.2.3. Third Eyelid

The histological study of the third eyelid (Figures 9 and 10) revealed notable differences between the two species under investigation, particularly in the degree of tissue development between the wolf (Figure 10A–D) and the domestic dog (Figure 10E–H) Differences in epidermal development between the two species are evident. The dog has a thicker epithelium and stronger PAS and Alcian Blue staining than the wolf. Cartilaginous tissue

exhibited strong staining with all four techniques in both species (Figures 9A,C and 10A,C), with no appreciable differences between them.

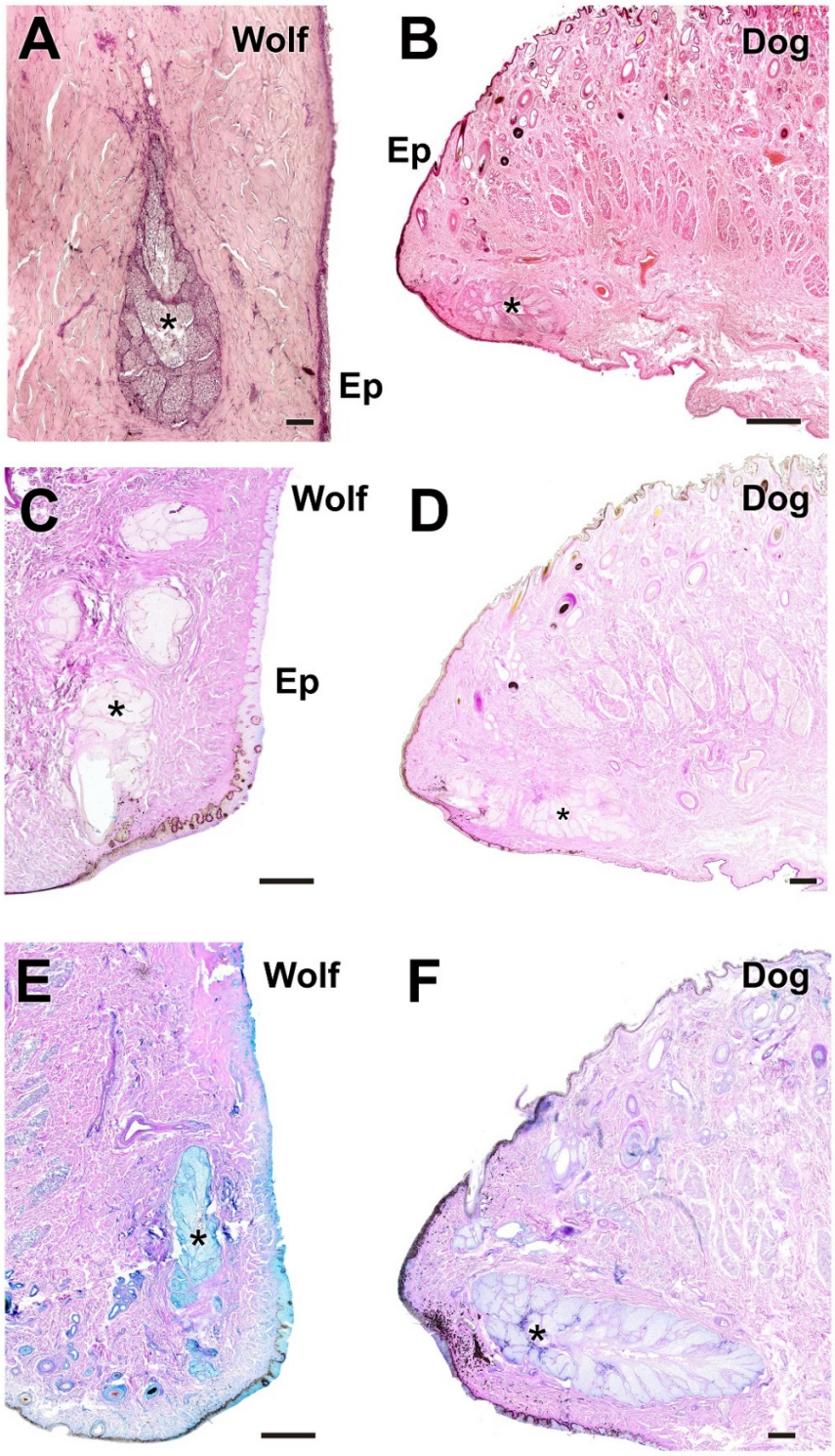

Figure 7. Histological images of dog and wolf upper eyelids stained with hematoxylin–eosin, PAS, and PAS-AB. They show the main glandular elements of the dog (**B**,**D**,**F**) and wolf (**A**,**C**,**E**) upper eyelid, the tarsal glands (*). Ep, epidermis. Histological stains: Hematoxylin–eosin (**A**,**B**); PAS (**C**,**D**); PAS-AB (**E**,**F**). Scale bars: (**A**,**D**,**F**) = 100 µm; (**B**,**C**,**E**) = 500 µm.

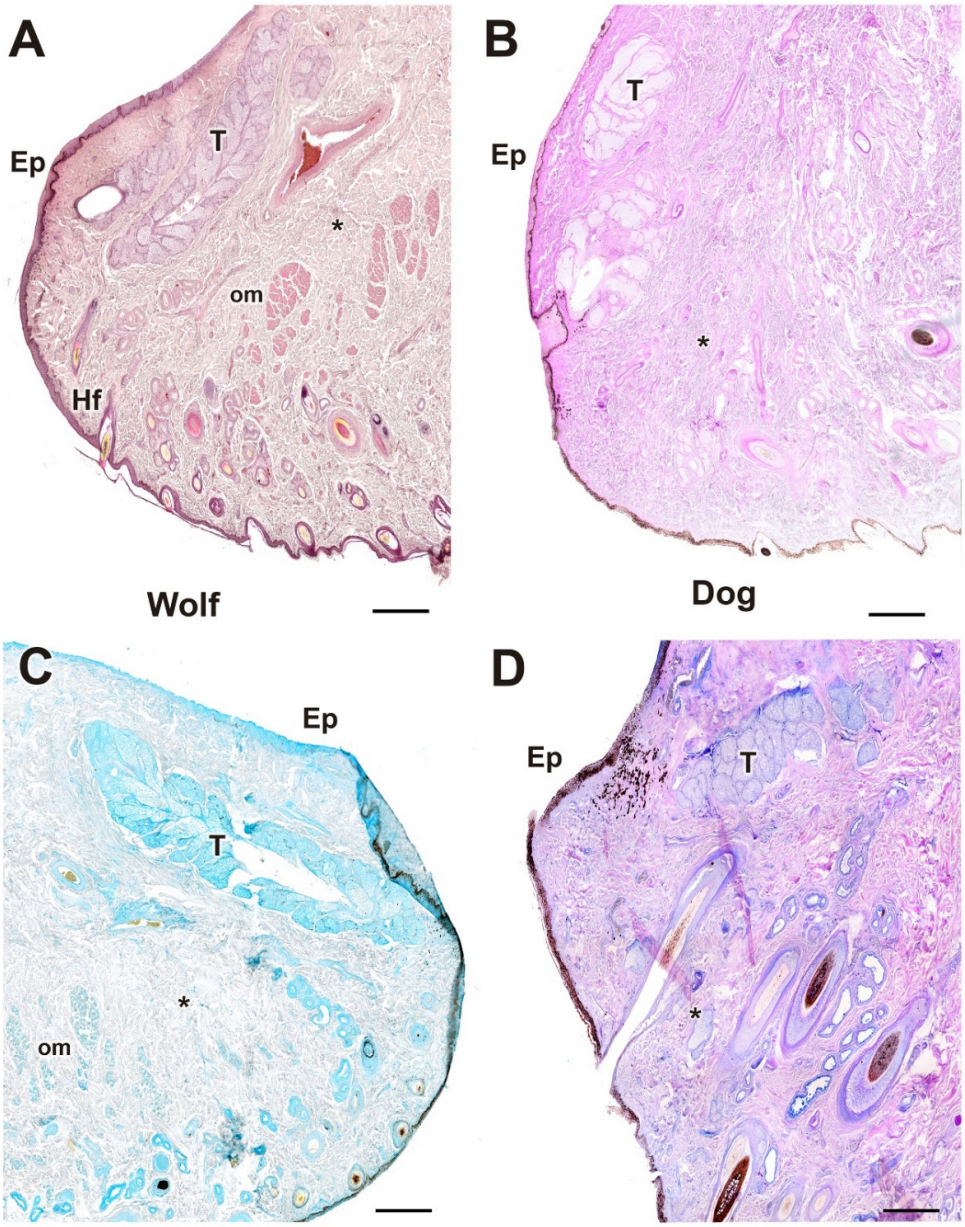

Figure 8. Histological images of the dog's and wolf's lower eyelids stained with hematoxylin–eosin, PAS, AB, and PAS-AB. The four histological stains used ((**A**), hematoxylin–eosin; (**B**), PAS; (**C**), AB; (**D**), PAS-AB) allow identification of the main glandular elements of the dog's (**B**,**D**) and wolf's (**A**,**C**) lower eyelids: Ep, epidermis; T, tarsal gland; *, connective tissue. Scale bar: (**A**–**D**) = 100 µm.

3.2.4. Tarsal Glands

The tarsal glands in the four stains did not show noticeable differences in parenchymal organization (Figure 11). However, dogs showed a prominent development of the tarsal gland lumen (Figure 11D), while wolves exhibited additional aggregates of tarsal glandular lobules (Figure 11B). In both species, the glandular secretion was acidic and Alcian Blue-positive (Figure 11A,E) but PAS-negative. In contrast, PAS strongly stained the collagen fibers of the surrounding connective tissue (Figure 11B,F). In wolves, aggregates of up to three tarsal lobules were frequently observed (Figure 11B).

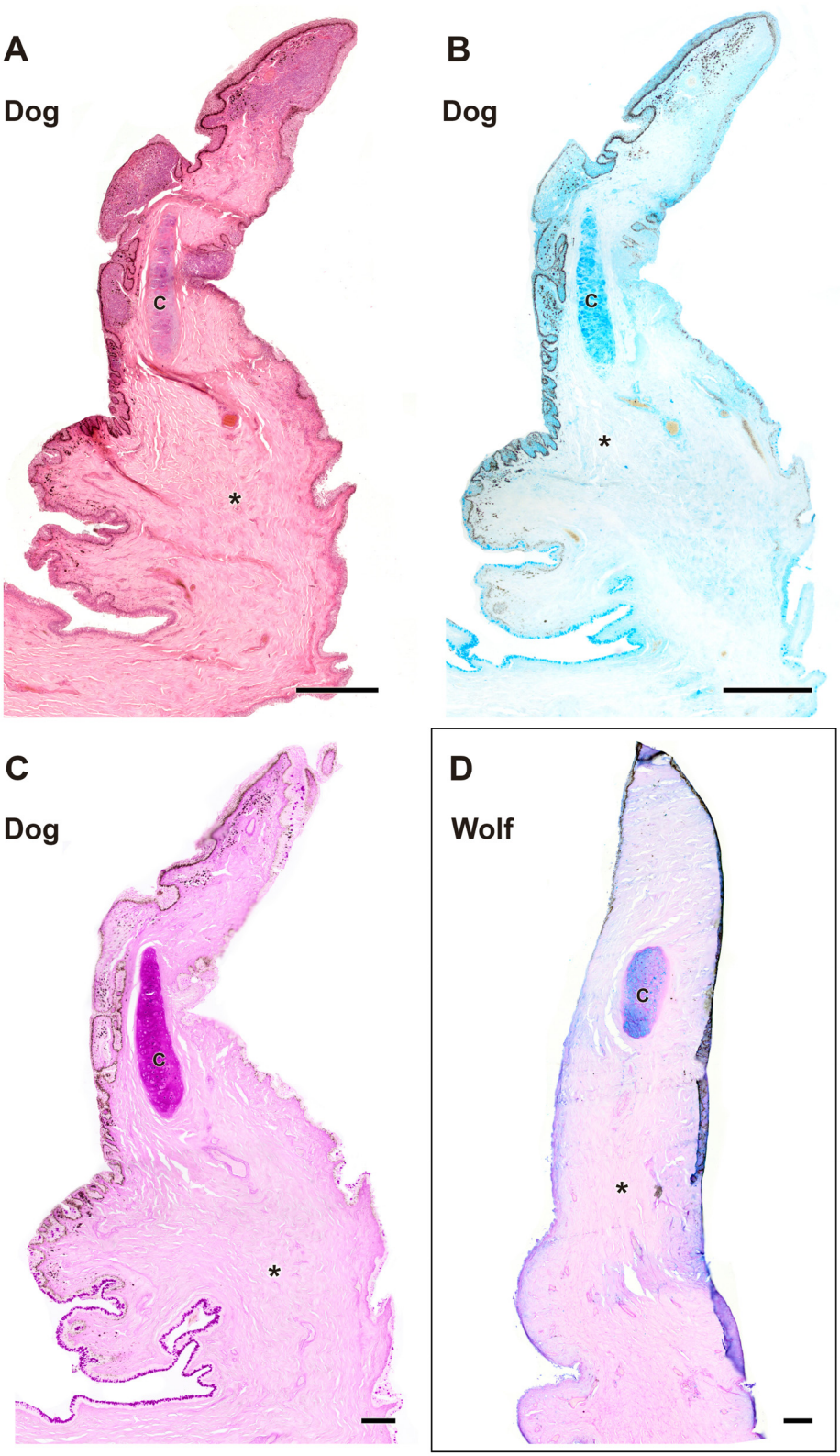

Figure 9. Complete histological sections of the third eyelid of the wolf and dog. The stains used ((**A**), Hematoxylin-eosin; (**B**), AB; (**C**), PAS; (**D**), PAS-AB) allow recognition of the cartilaginous skeleton, connective tissue development, and epithelial lining epithelia of the bulbar and palpebral surface of the dog (**A**–**C**) and wolf (**D**): C, cartilage; *, connective tissue. Scale bar: (**A**,**B**) = 500 µm; (**C**,**D**) = 100 µm.

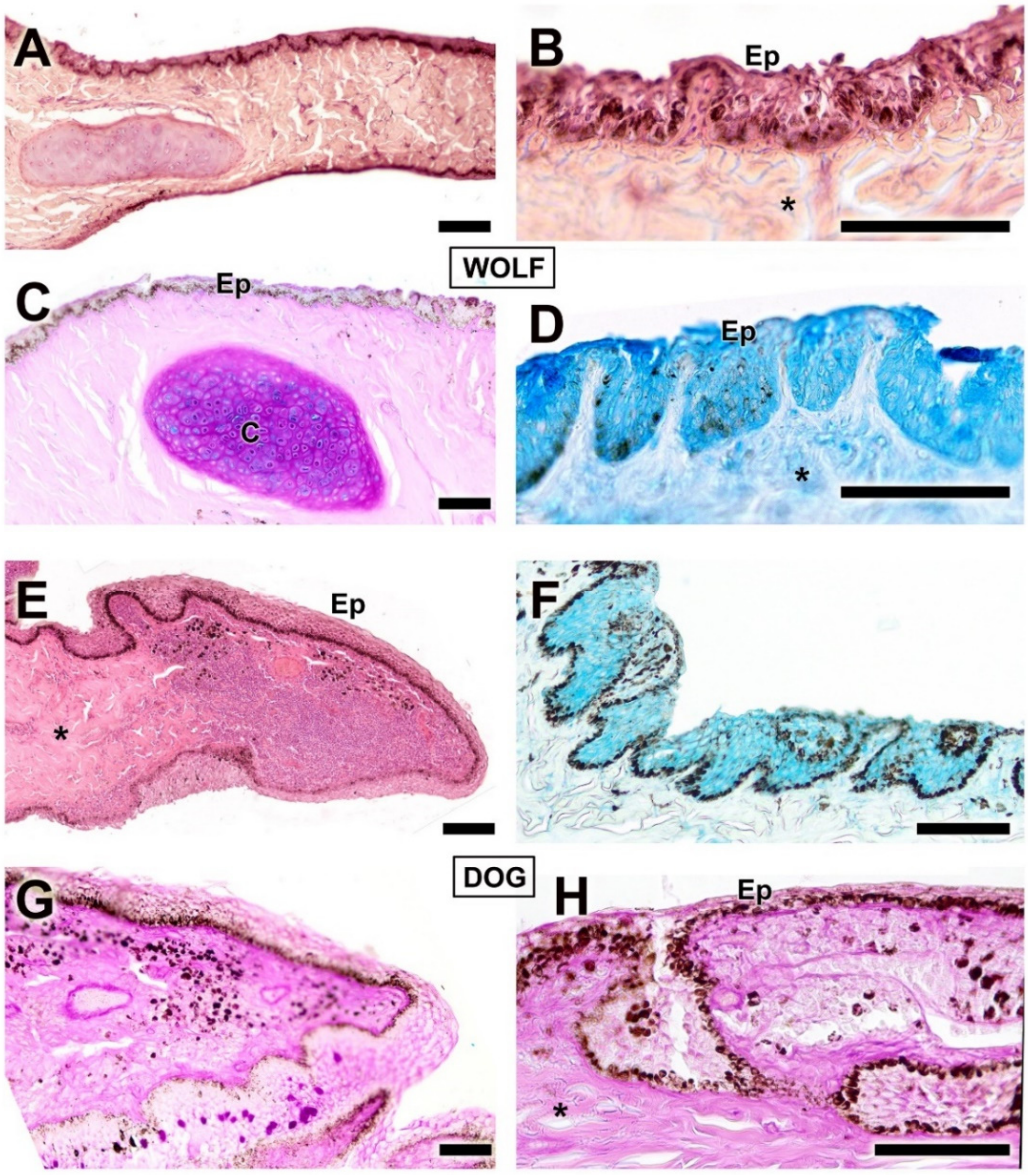

Figure 10. Histological transversal sections of the third eyelid of the dog and wolf. The different degrees of development between the epidermis of both species can be appreciated. (**C**), cartilage; Ep, epidermis; *, connective tissue. Histological stains used: (**A**,**B**,**E**) Hematoxylin–eosin; (**C**,**G**,**H**) PAS; (**D**,**F**) AB. Scale bar: (**A**–**H**) = 100 µm.

3.2.5. Palpebral Conjunctiva, Bulbar Conjunctiva, and Fornix

The histological study of the palpebral conjunctiva, bulbar conjunctiva, and fornix reveals intense staining in both epithelial types in the dog using Alcian Blue and hematoxylin–eosin. The conjunctiva exhibits strong pigmentation and prominent deep tubular invaginations in the palpebral conjunctiva (Figure 12A,B). In dogs, the palpebral mucosa is notably thick (Figure 13A) and exhibits strong expression of both neutral (Figure 13B) and acidic mucopolysaccharides (Figure 13C).

In the wolf, acidic mucopolysaccharides were predominant in both the palpebral conjunctiva (Figure 13D) and the fornix (Figure 13F); this is not the case in the dog, where the fornix primarily expresses neutral mucopolysaccharides (Figure 13E) within both the connective tissue and the unicellular mucous glands.

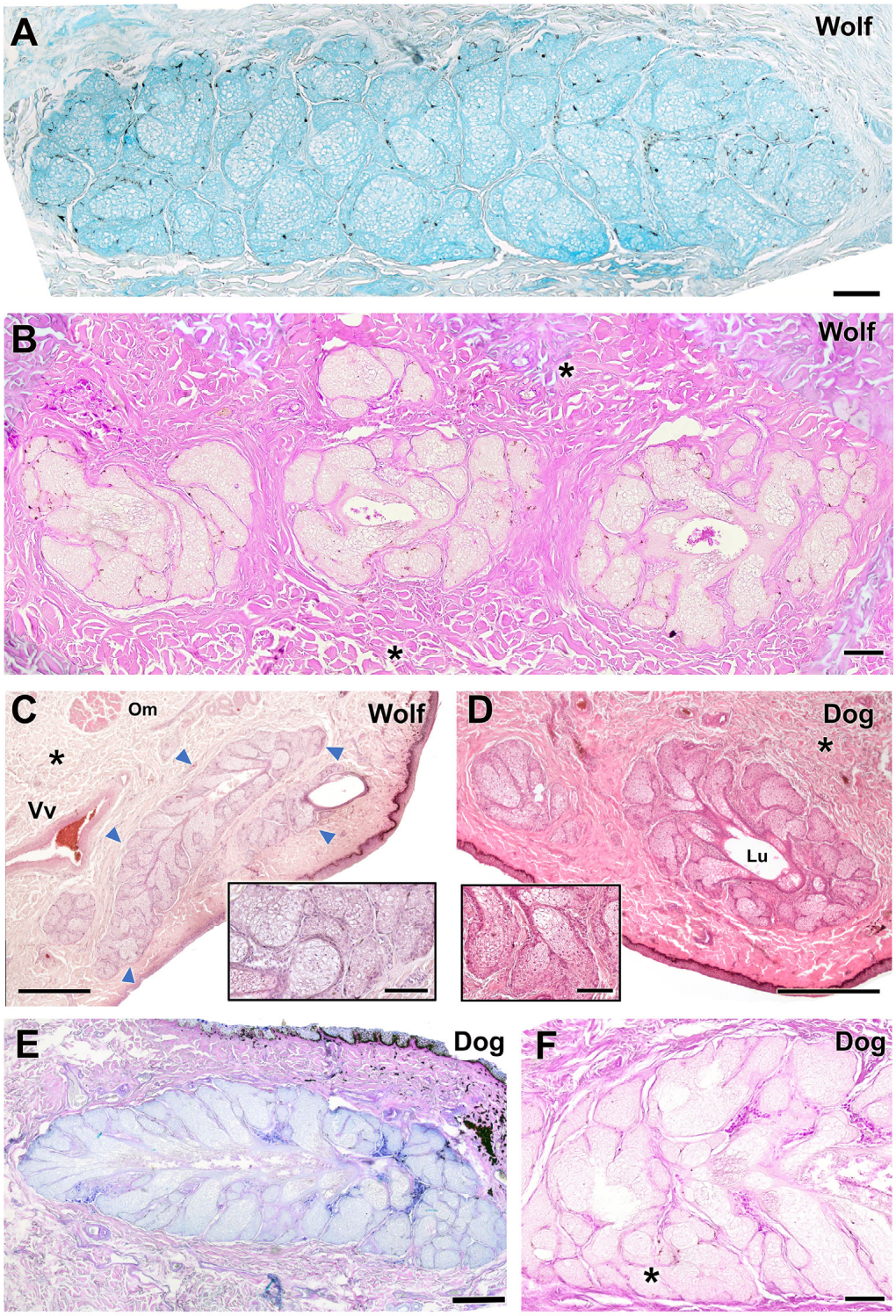

Figure 11. Histological study of the tarsal gland of the dog and wolf. In both species, wolf (**A**,**B**) and dog (**E**,**F**), the glandular secretion is acidic in nature, Alcian Blue-positive (**A**,**E**), and PAS-negative (**B**,**F**). (**C**,**D**) Hematoxylin–eosin staining reveals extensive development of the tarsal gland (arrowheads) in both wolf (**C**) and dog (**D**), with no striking differences. Only in the case of the dog does the large development of the lumen (Lu) stand out. In both species, the tarsal gland is negative for PAS staining, which, however, strongly stains the collagen fibers that form the surrounding connective tissue (asterisks). In the case of the wolf, the presence of aggregates of up to three lobes of tarsal glandular tissue is striking (**B**). Om, orbicularis muscle; Vv, veins. Staining: (**A**), AB; (**B**,**F**), PAS; (**C**,**D**), hematoxylin–eosin; (**E**), PAS-AB. Scale bar: (**C**–**F**) = 500 µm; (**A**,**B**) = 100 µm.

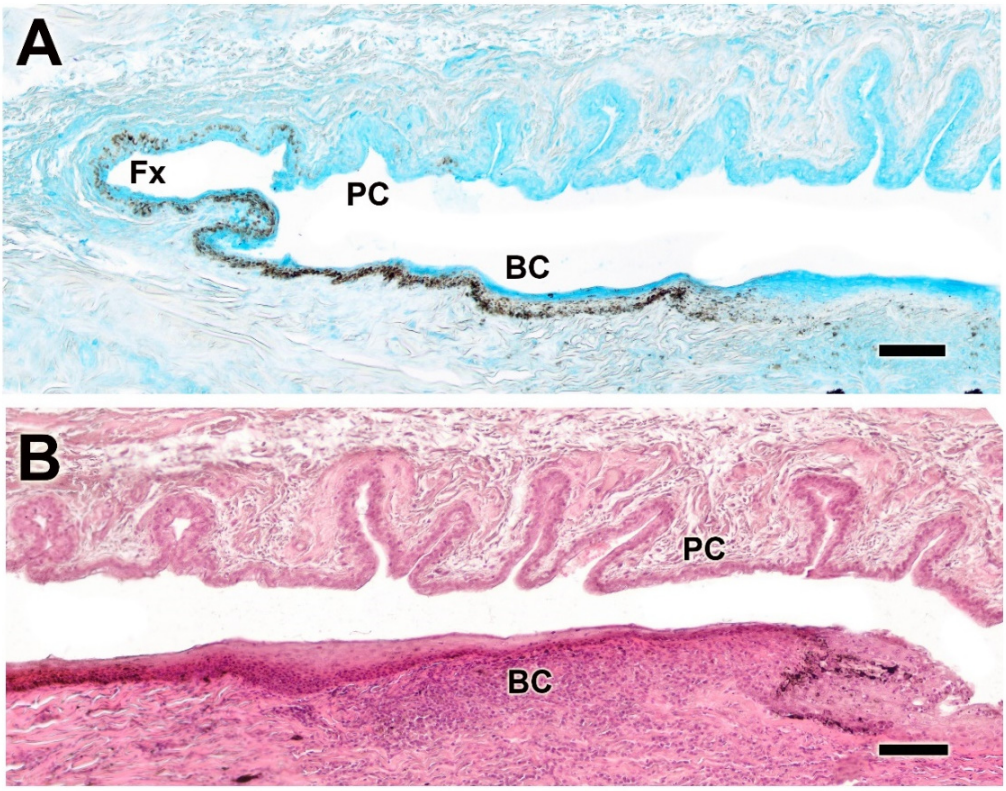

Figure 12. Histological study of the bulbar, palpebral, and fornix conjunctivae of the dog. (**A**). Alcian Blue staining shows intense staining of the epithelial lining, which is heavily pigmented and forms deep tubular invaginations. (**B**) Histological image stained with hematoxylin–eosin reveals a remarkable development of these glandular formations, particularly at the level of the palpebral conjunctiva. BC. bulbar conjunctiva; Fx, fornix; PC, palpebral conjunctiva. Scale bar: (**A**,**B**) = 100 µm.

The bulbar conjunctiva of the dog (Figure 14) consists of a well-developed stratified squamous epithelium (Figure 14A,B) that exhibits strong PAS-negativity and slight AB positivity (Figure 14A), which contrasts with the wolf. The latter displays markedly reduced epithelial thickness and intense AB positivity (Figure 14C) and slight PAS reactivity, predominantly on the luminal surface (Figure 14D).

3.2.6. Cornea

The histological study of the cornea did not reveal noticeable differences between the dog and wolf (Figure 15); however, it enables the identification of the distinct layers comprising the cornea (Figure 15B–D). PAS and AB staining exhibited similar histochemical patterns with more intense stromal staining (Figure 15D,E).

3.2.7. Ciliary Body

The ciliary body is histologically very similar in both species and does not show appreciable morphological differences when stained with hematoxylin–eosin, Alcian Blue, and PAS–Alcian Blue in either the wolf (Figure 16A–C) or the dog (Figure 16D–E). However, these stains allow us to observe in detail components such as the ciliary stroma (Figure 16A), the ciliary processes (Figure 16A–E), and the two epithelial layers (Figure 16B–C): a pigmented epithelium, which displays the same degree of pigmentation in both species, and an overlying non-pigmented epithelium, which shows weak reactivity to both Alcian Blue and PAS in the wolf (Figure 16B,C).

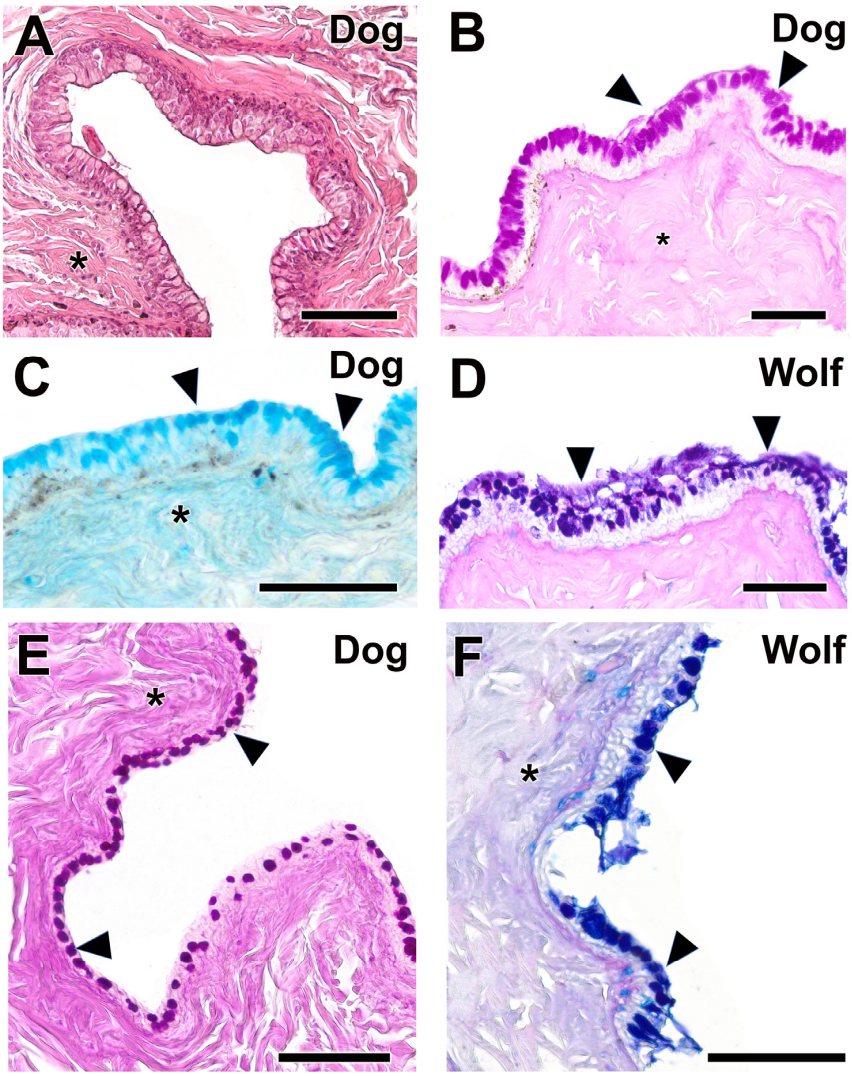

Figure 13. Histological study of palpebral conjunctiva and fornix in the dog and wolf. (**A**). Hematoxylin–eosin shows the remarkable thickness of the palpebral mucosa in the dog. (**B**,**C**). This morphological development corresponds with a remarkable expression of neutral (**B**) and acidic (**C**) mucopolysaccharides (arrowheads). (**D**,**F**). In the wolf, expression of acidic polysaccharides predominates in both the PC (**D**) and the fornix (**F**). (**E**). The dog fornix shows a remarkable expression of neutral mucopolysaccharides, both in the unicellular mucous glands and in the submucosal connective tissue (*). Stains: (**A**). Hematoxylin–eosin; (**B**,**E**). PAS; (**C**). AB; (**D**,**F**). PAS-AB. Scale bar: (**A**–**F**) = 100 µm.

3.2.8. Tunics of the Eye

This histological study, conducted using hematoxylin–eosin staining, elucidated the organization of the three principal tunics in the canine eye (Figure 17A), delineated the various strata comprising the retina in both species (Figure 17B,C), and characterized the morphology of the choroid in the wolf (Figure 17D). The retinal layers are organized as follows: 1—Outermost pigmented epithelium; 2—Cone and rod layer; 3—Outer limiting layer, consisting of junctions between photoreceptor cells and Müller cells; 4—Outer nuclear layer, containing nuclei of photoreceptor cells; 5—Outer plexiform layer, a junctional zone between photoreceptor and bipolar cells; 6—Inner nuclear layer, containing nuclei of amacrine, bipolar, and horizontal cells; 7—Inner plexiform layer, a connectivity area among ganglion, amacrine, and bipolar cells; 8—Ganglion cell layer; 9—Optic nerve fiber layer (axons of ganglion cells); 10—Internal limiting layer, primarily serving to separate the retina from the vitreous humor.

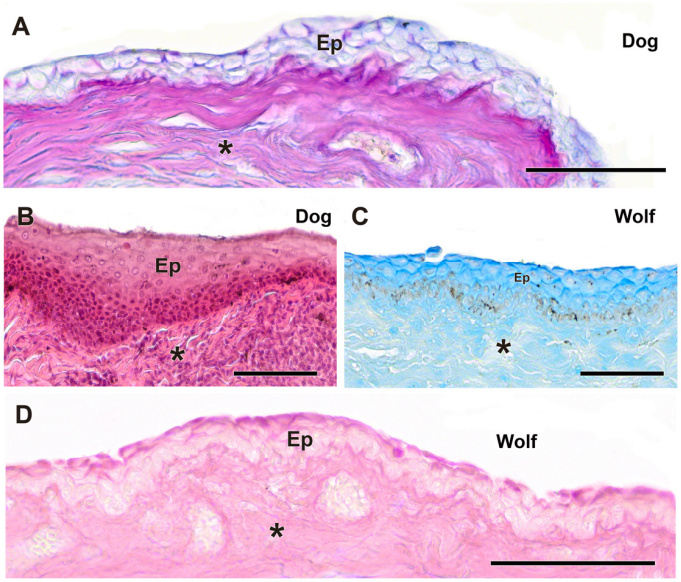

Figure 14. Histological study of the bulbar conjunctiva in the dog and wolf. (**A**,**B**) In the dog, the remarkable development of the stratified squamous epithelium is evident. The bulbar conjunctiva of the dog also shows a strong AB-positive reaction and a negative reaction to PAS (**A**). (**C**,**D**). In the wolf, the epithelium is thinner and exhibits an intense positive reaction to AB (**C**). (**C**). The wolf bulbar conjunctiva shows a certain reactivity to PAS, particularly on its luminal surface (**D**). Ep. Epidermis; *. Connective tissue. Staining: (**A**). Hematoxylin–eosin; (**B**). AB; (**C**). PAS-AB; (**D**). PAS. Scale bar: (**A**–**D**) = 100 µm.

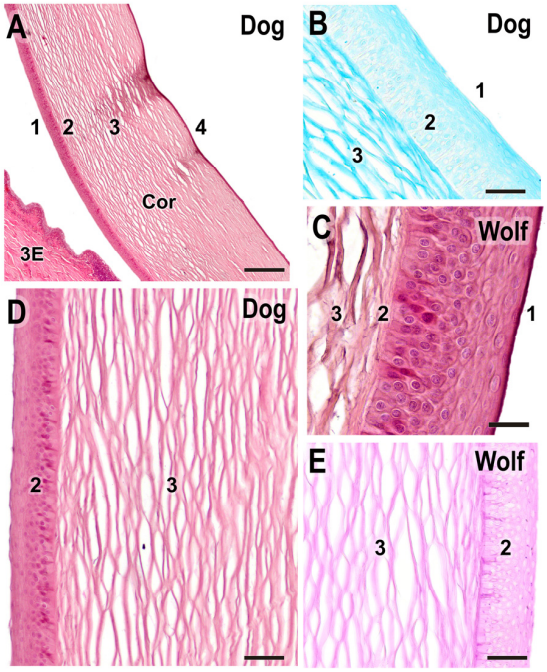

Figure 15. Histological study of the cornea. (**A**). General structure of the dog cornea showing the distinct strata: (1) epithelium, (2) Bowman's layer, (3) stroma, and (4) Descemet's membrane. (**B**). Alcian Blue staining of the dog cornea, highlighting the intense staining of the stromal matrix (3), along with the epithelium (1) and Bowman's layer (2). (**C**). Superficial corneal strata of the wolf, showing the epithelium (1), Bowman's layer (2), and beginning of the stroma (3). (**D**). Histological structure of the superficial corneal strata in the dog. (**E**). PAS staining in the wolf cornea. 3E, third eyelid; Cor, cornea; 1. anterior epithelium; 2. anterior limiting lamina (Bowman's layer); 3. corneal stroma; 4. posterior limiting lamina (Descemet's membrane) + posterior epithelium. (**A**,**C**,**D**). H-E; (**B**). AB; (**E**). PAS. Scale bar: (**A**) = 500 µm; (**B**–**E**) = 100 µm.

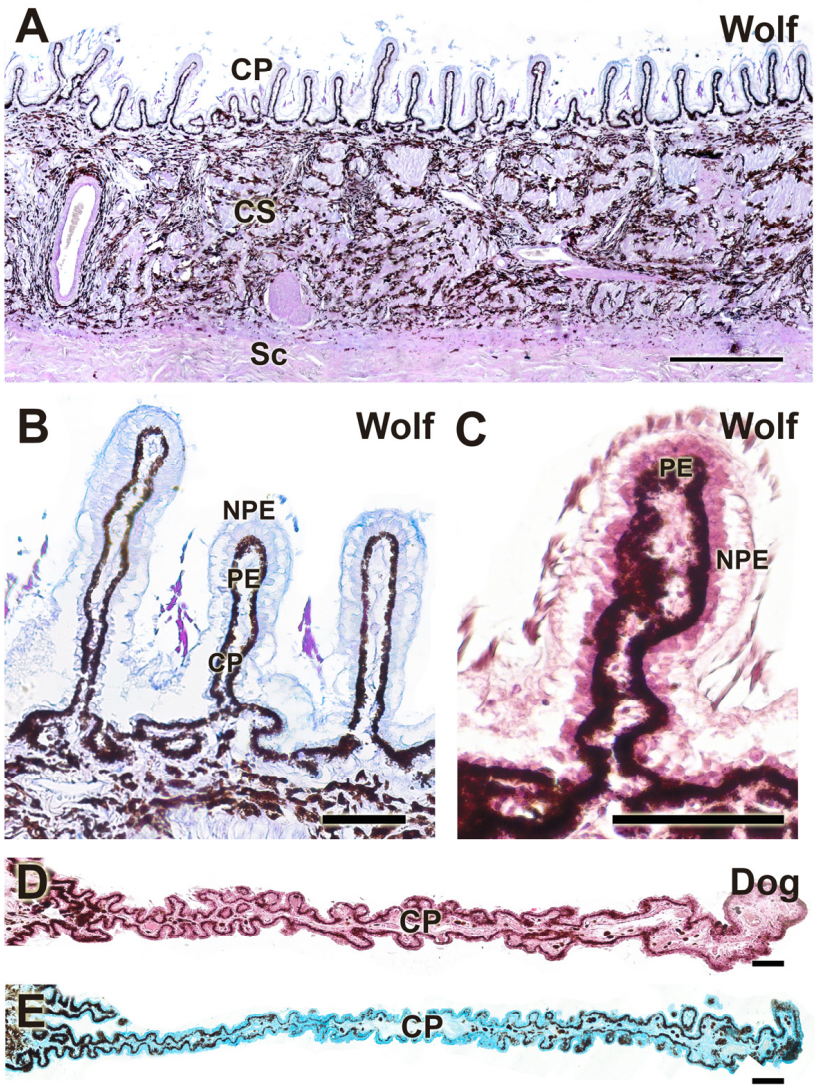

Figure 16. Histological study of the ciliary body. Structurally, there are no appreciable differences between the wolf (**A**–**C**) and the dog (**D**,**E**). CP, ciliary process; CS, ciliary stroma; NPE, non-pigmented epithelium; PE, pigmented epithelium; Sc, Sclera. Stains: (**A**): PAS-AB; (**B**,**E**): H-E; (**C**): AB; (**D**): PAS-AB. Scale bar: (**A**) = 500 µm; (**B**–**E**) = 100 µm.

3.2.9. Lacrimal Gland

In the histological analysis performed with hematoxylin–eosin staining, we examined the morphological organization of the lacrimal gland in the wolf. Particular attention was given to the lacrimal duct, which is surrounded by adipose tissue (Figure 18A), and to the detailed structure of the glandular parenchyma at higher magnification (Figure 18B).

3.3. Lectin Histochemical Study

The histochemical analysis of the canine palpebral complex, conducted using UEA lectin (Figure 19), revealed more intense and specific labeling, particularly in the tarsal glands of both the upper and lower eyelids, with similar intensity in each. Additionally, strong labeling was observed in the mucosal epithelial lining of the upper eyelid, lower eyelid, and third eyelid. Notably, the third eyelid exhibited a marked reaction along both of its epithelial layers, characterized by prominent pits containing UEA-positive tubular glands (Figure 20B).

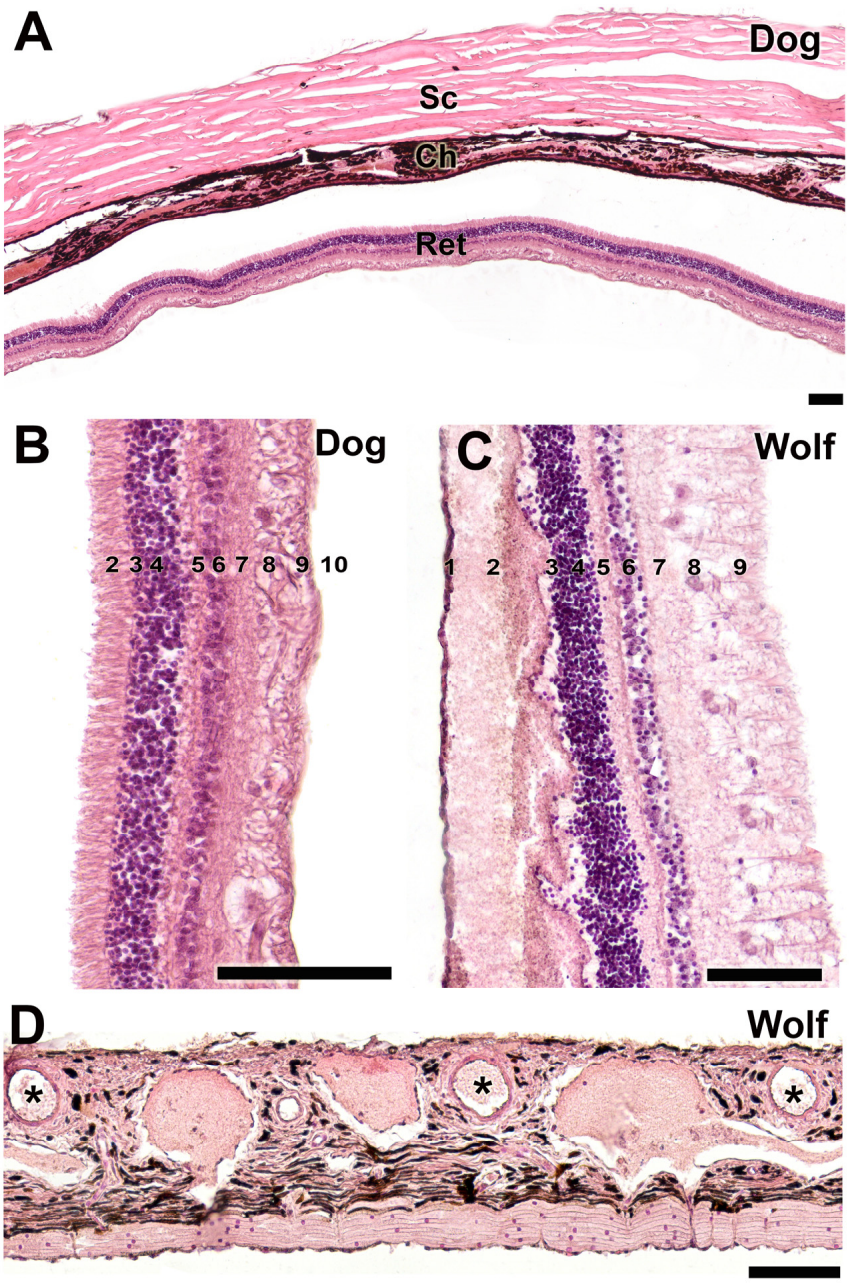

Figure 17. Histological study of the sclera, choroid, and retina. (**A**). Organization of the three fundamental tunics of the eye in the dog. Strata that make up the retina of the dog (**B**) and wolf (**C**). 1. pigmented epithelium; 2. cone and rod layer; 3. outer limiting membrane; 4. outer nuclear membrane; 5. outer plexiform membrane; 6. inner nuclear membrane; 7. inner plexiform membrane; 8. ganglion cells; 9. optic nerve fibers; 10. inner limiting membrane. (**D**). Choroid of the wolf. Ch, choroid; Ret, retina; Sc, sclera; *, blood vessels. Staining: Hematoxylin–eosin. Scale bar: (**A**–**D**) = 100 μm.

Similarly, the UEA lectin labeling pattern in the wolf eye showed no remarkable differences compared to that observed in the dog, highlighting a specific and strong reaction in the skin, palpebral conjunctiva, tarsal glands, and third eyelid (Figure 20D–F).

In contrast, LEA lectin results differed between species, showing a differential labeling pattern. A notably intense reaction was observed in the tarsal gland of the canine eye (Figure 20A), whereas a weaker signal was observed in the tarsal gland of the wolf (Figure 20C). A comprehensive summary of the obtained results is presented in Table 1.

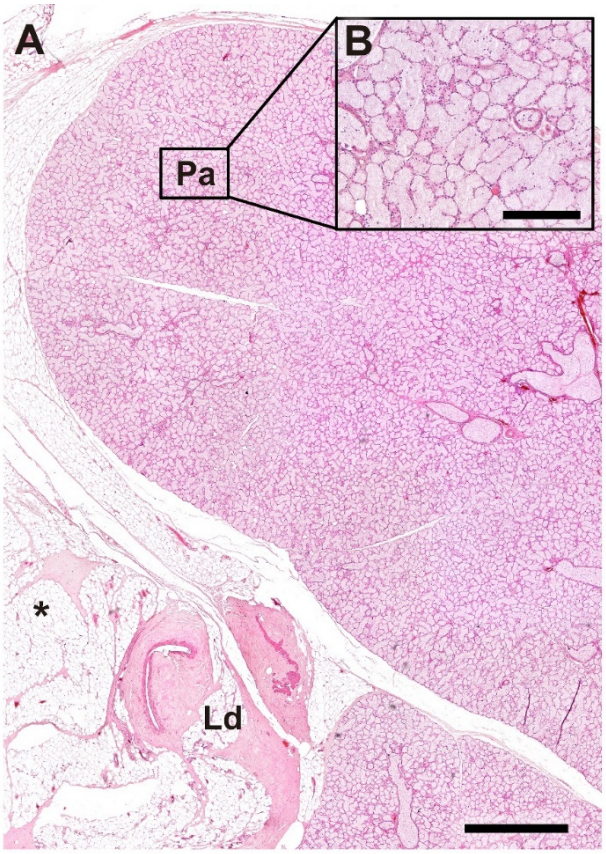

Figure 18. Histological structure of the lacrimal gland of the wolf. (**A**). General microscopic view of the gland. (**B**). Image of the parenchyma at higher magnification. Ld, lacrimal duct; Pa, Parenchyma; *, Adipose tissue; Stain: H-E. Scale bar: (**A**) = 500 μm; (**B**) = 100 μm.

Table 1. Summary of histological and lectin–histochemical findings in the ocular adnexa of dogs and wolves.

Structure	Dog	Wolf	Appreciable Difference
Eyelid Skin lining	Histology: Non-keratinized stratified squamous epithelium; abundant superficial dermal glands	Histology: Same epithelial type; fewer dermal glands	Greater glandular density in the dog
	Lectin: Strong UEA lectin labeling in skin, palpebral conjunctiva	Lectin: Similar strong UEA lectin labeling in skin, palpebral conjunctiva	No difference in UEA labeling pattern
Upper and lower eyelids	Histology: Well-developed; Meibomian, Moll, and Zeis glands; dense collagen; more elastic due to richer connective tissue	Histology: Similar structure; dense collagen; less connective tissue, more fibrous	Greater elasticity and connective tissue in the dog
	Lectin: Strong UEA lectin labeling in upper and lower eyelid mucosal epithelia	Lectin: Similar strong UEA lectin labeling in upper and lower eyelid mucosal epithelia	No difference in UEA labeling pattern
Third eyelid	Histology: Thicker epithelium; stronger PAS and AB staining (more secretory activity)	Histology: Thinner epithelium; weaker PAS and AB staining	More developed epithelium and secretory activity in the dog
	Lectin: Intense UEA lectin labeling along both lining epithelia; UEA-positive pits with tubular glands	Lectin: Similar intense UEA lectin labeling in the lining epithelia and tubular glands	No difference in UEA lectin pattern
Tarsal glands	Histology: Similar parenchymal structure; larger glandular lumen	Histology: Similar parenchymal structure; more frequent glandular aggregates (up to 3 lobes)	Dog: larger lumens; Wolf: more glandular lobes

Table 1. *Cont.*

Structure	Dog	Wolf	Appreciable Difference
Tarsal glands	Lectin: Intense UEA and strong LEA lectin labeling	Lectin: Intense UEA but weak LEA lectin labeling	LEA lectin labeling is markedly weaker in the wolf
Palpebral, bulbar conjunctiva, and fornix	Thick palpebral mucosa; deep tubular invaginations; strong PAS and AB staining; well-developed bulbar epithelium with negative PAS, mild AB staining	Strong AB in fornix and palpebral mucosa; thin bulbar epithelium with slight PAS staining and strong AB.	Dog: thick epithelium, more neutral mucins; Wolf: thin epithelium, more acidic mucins
Cornea	Typical layered structure; stroma stains strongly with AB	Same layered structure; stroma stains strongly with PAS	No differences
Ciliary body	Similar morphology; pigmented and non-pigmented epithelia; low PAS/AB reactivity	Similar morphology; pigmented and non-pigmented epithelia; low PAS/AB reactivity	No morphological differences
Ocular tunics and retina	Typical three tunics; detailed retinal layering observed	Greater density of ganglionar cells in the retina. Same tunic organization	Greater density of ganglionar cells in the retina of the wolf
Lacrimal gland	Morphology not detailed in the current data	Well-organized glandular parenchyma; lacrimal duct surrounded by adipose tissue	Detailed description available only for the wolf

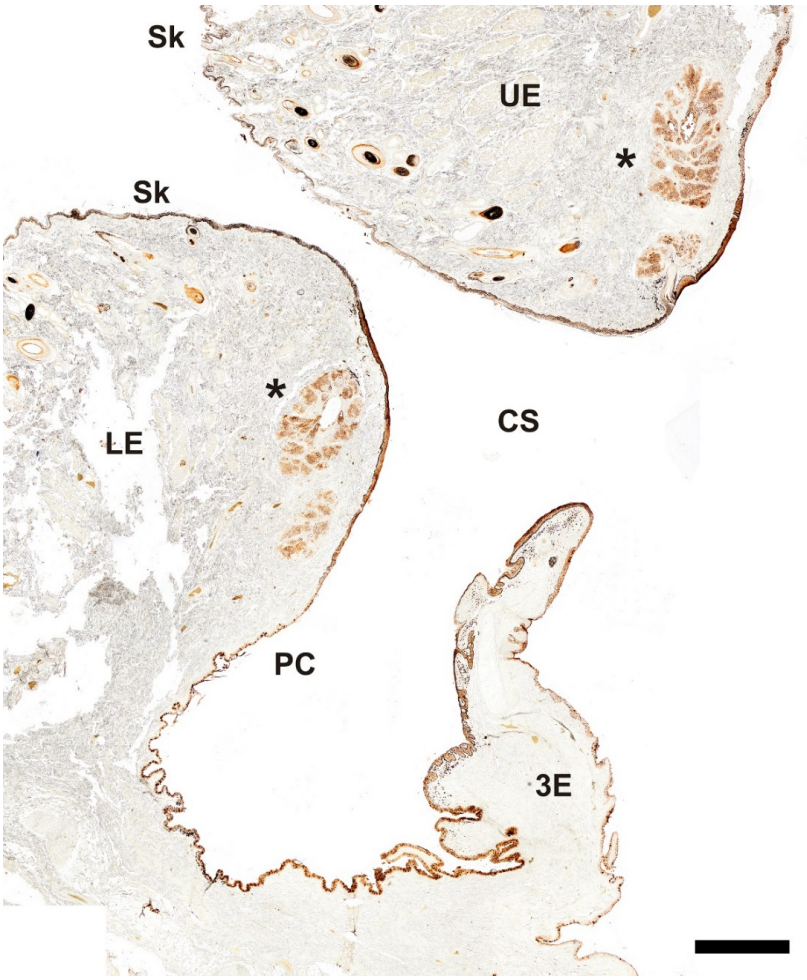

Figure 19. Histochemical study of the palpebral complex of the dog using UEA lectin. The lectin specifically labels the tarsal glands of the upper and lower eyelid, palpebral mucosal linings, and hair follicles. 3E, third eyelid; CS, conjunctival sac; LE, lower eyelid; PC, palpebral conjunctiva; Sk, skin; UE, upper eyelid; *, tarsal glands. Scale bar = 500 μm.

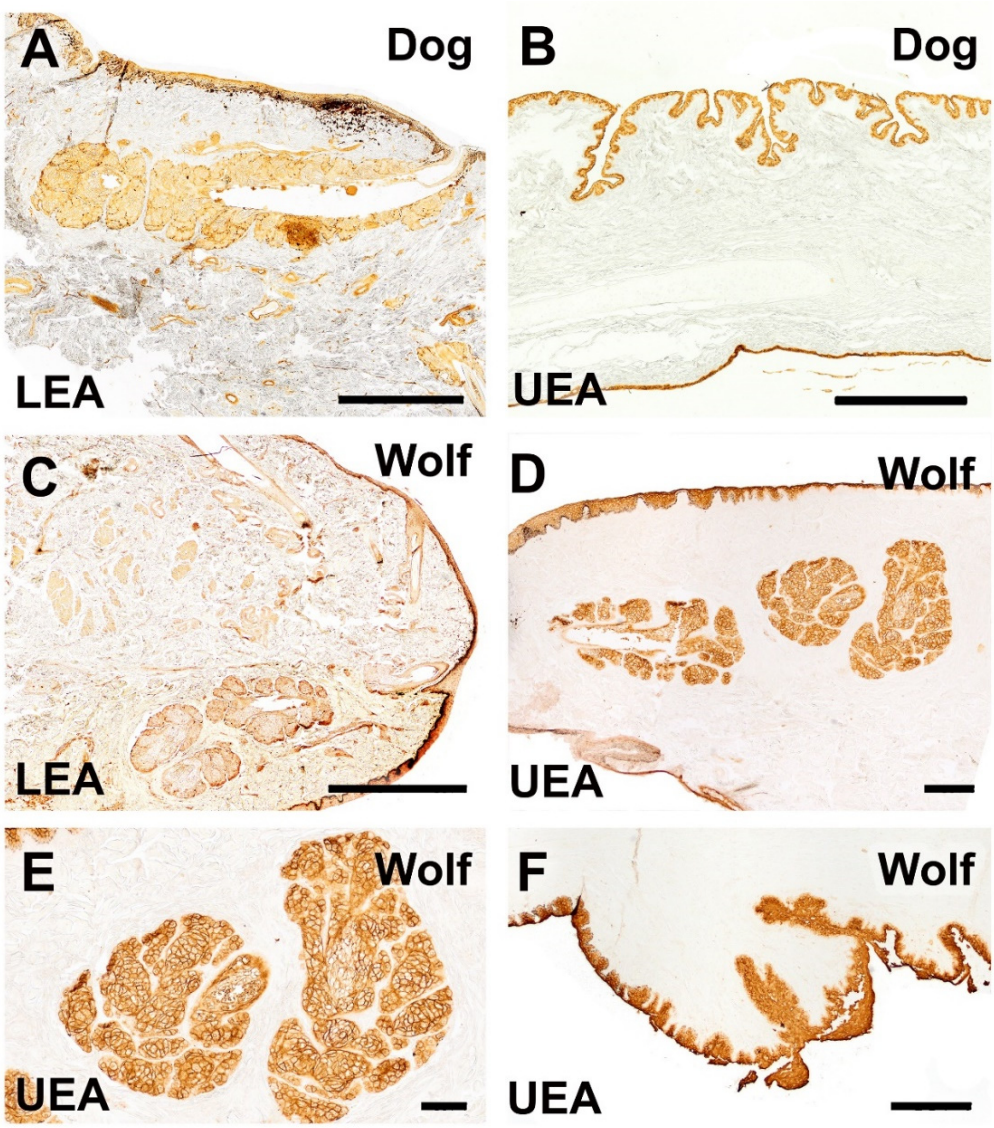

Figure 20. Histochemical study of the dog and wolf eyelids using LEA and UEA lectins. (**A**,**C**). LEA lectin exhibits differential labeling between the two species, demonstrating a strongly intense reaction in the tarsal gland of the dog and a very weak reaction in that of the wolf. (**B**). A cross-section of the third eyelid of the dog reveals an intense reaction in its two lining epithelia. Notably, in the palpebral lining, the presence of pits opening into UEA-positive tubular glands is prominent. (**D**–**F**). In the wolf, UEA lectin displays a labelling pattern similar to that observed in the dog, with an intense and specific reaction in the skin, palpebral conjunctiva, tarsal glands (shown at higher magnification in (**E**)), and the third eyelid (**F**). Lectins: (**A**,**C**). LEA; (**B**,**D**–**F**): UEA. Scale bar (**A**–**C**,**F**) = 500 µm; (**D**,**E**) = 100 µm.

4. Discussion

We conducted a comprehensive histological and histochemical comparison of the canine and wolf eyes, focusing on glandular structures relevant to ocular pathologies such as KCS [33,34]. This study, which includes the first detailed description of the wolf's ocular adnexa, provides new insights into anatomical changes potentially linked to domestication and has implications for both conservation and translational research. This detailed histological and histochemical description of the wolf's eye provides novel insights, describing for the first time the characteristics of the eye and its appendages in this species. The wolf (*Canis lupus signatus*) is listed on the IUCN Red List [35], underscoring the importance of studying its anatomy and physiology to increase conservation efforts. Common ocular

diseases among wild canids include conjunctival and corneal pathologies and dry eye syndrome, all of which are associated with deficiencies in the aqueous tear component [13,34]. These conditions, similar to those observed in domestic dogs [36–39], may exacerbate the ecological challenges faced by wolves, underscoring the need for anatomical knowledge of the glandular system. From a translational perspective, our research bridges the gap between basic studies and clinical practice, contributing to the advancement of human ocular pathology research. As animal models, domestic dogs are more similar to humans than traditional laboratory animals, such as mice, particularly in terms of ocular anatomy and physiology.

Extensive anatomical studies have been conducted on the ocular system of dogs, including macroscopic and morphometric characterization of the lacrimal and third eyelids [11], individual analysis of the lacrimal glands [40,41], evaluation of the cornea and conjunctiva [33], identification of the nictitating membrane [42], and characterization of goblet cells [7,43–45]. In this context, our study provides an integrated, comparative histological and histochemical analysis of the ocular surface and adnexa of dogs and wolves.

Our macroscopic study confirmed the similarity of the dog and wolf eyeball structures. We assessed the outer tunic, formed by the sclera and cornea; the middle tunic, comprising the choroid, iris, and ciliary body; and the inner tunic formed by the parts of the blind and optical areas of the retina. Furthermore, we examined the three chambers: anterior, posterior, and vitreous. The histological organization of the three ocular tunics was consistent with prior descriptions in dogs [46]. Microscopic examination of the eyelids revealed nonkeratinized stratified squamous epithelium, hair follicles, and underlying connective tissue in both species, which aligns with prior descriptions in African wild dogs (*Lycaon pictus*) [47] and black bears (*Ursus thibetanus*) [47]. The glandular analysis revealed the presence of tarsal Moll's and Zeis glands. African wild dogs exhibit a stratified squamous epithelium with 9 to 13 layers of nucleated cells and elongated tarsal vesicular glands (more developed in the upper eyelids); furthermore, the stroma of both eyelids exhibits dense and irregular connective tissue, with a network of collagen and elastic fibers [47]. This structure aligns with our observations in dogs and wolves; the former species exhibits more developed connective tissue, explaining its greater elasticity compared to that of the wolf, which is more fibrous. The African wild dog may represent an evolutionary intermediate between the wolf and the domestic dog [48]. Additionally, dogs exhibit a thicker epithelium than wolves, exhibiting greater PAS and Alcian Blue-positive secretions than wolves. The cornea and ciliary body show no notable differences between the studied species.

Histological analysis of the palpebral and bulbar conjunctiva revealed strong pigmentation and numerous deep tubular invaginations in dogs, which aligns with studies quantifying goblet cell densities [44,49]. The canine bulbar conjunctiva exhibited a highly developed stratified squamous epithelium with intense PAS-negative and Alcian Blue-positive reactions, differing from those of the wolf, which displayed a thinner epithelium with PAS reactivity mainly on the luminal surface. At the retinal level, our observations revealed a noticeably greater density of ganglion cells in the wolf than in the dog, a finding that aligns with previous topographic studies by Peichl and collaborators, who described a more prominent area centralis and denser retinal ganglion cell population in the wolf [50–52].

At the cutaneous level, both the dog and the wolf display the same nonkeratinized stratified squamous epithelium, hair follicles, and connective tissue that covers the eyelids. However, dogs possess a greater number of glandular components near these areas than wolves. Notably, dogs exhibit more developed connective tissue than wolves, in which this tissue is more fibrous, potentially explaining the greater elasticity of this tissue in dogs and the ease of eyelid surgery in this species. These findings align with prior suggestions of

evolutionary divergence between domestic dogs and their wild ancestors, specifically in the context of comparative ophthalmology [34]. Increased eyelid elasticity may contribute to enhanced protective and expressive functions of the eye in some domestic dogs. Indeed, certain studies have noted the capacity of dogs to produce specific facial expressions when interacting with humans [53]. However, these traits are known to vary substantially across breeds, particularly in relation to head shape, skin structure, and soft tissue composition. From a veterinary perspective, the observed elasticity may facilitate surgical procedures by reducing resistance to incision and tissue trauma. Moreover, evolutionarily, this difference may reflect adaptations to domestic environments and the specific lifestyles of dogs, in contrast to wolves, which exhibit more fibrous and less elastic eyelids [54]. The facial musculature of dogs has been compared with that of humans, highlighting their shared muscular homology. This arrangement contrasts with that of the wolf, which, as previously mentioned, presents a more fibrous facial structure. This observation further supports the idea that dogs have undergone evolutionary differentiation due to their shared social environment with humans throughout history. Nevertheless, our findings are limited to three mesocephalic mixed-breed dogs, and further comparative studies across a broader range of breeds are necessary to obtain more general conclusions.

Lectins selectively bind to cellular surface glycoconjugates, which are involved in cell–cell interactions, such as differentiation, regulation, and tissue integrity [55]. The pattern of lectin binding sites differs not only between the same organs of different species but also within the organs of the same individual [23,56]. Some of these differences could correlate with various stages of cellular differentiation and organ development [57].

Our histochemical study using UEA lectin revealed strong and specific labeling in the tarsal glands of both the upper and lower eyelids, as well as in the mucosal epithelia of the upper, lower, and third eyelids. Labeling was particularly intense in the third eyelid, with prominent UEA-positive tubular gland pits. The staining pattern in the wolf was comparable to that in the dog, showing similar intensities in the skin, palpebral conjunctiva, tarsal glands, and third eyelid. In contrast, LEA lectin labeling differed between species, with strong reactivity in the dog and markedly weaker labeling in the wolf.

These findings align with previous observations of UEA binding in the anterior segment of the bovine eye [58], as well as in vitro studies using rabbit conjunctival epithelial cell cultures, where both LEA and UEA demonstrated strong and rapid binding to the ocular surface [59]. In contrast, Rittig et al. [60] reported that UEA-I binding in the human anterior eye segment is restricted to vascular endothelial cells and a limited subset of corneal and conjunctival epithelial cells. These findings suggest that lectin-based cell-typing or lectin labeling strategies may not be broadly applicable across species and should be interpreted with caution.

According to various authors [44], glycoconjugates are either absent or present at very low levels on the perilimbal bulbar conjunctiva in both dogs and humans. In contrast, glycoconjugates are more abundant in the lower nasal fornix, lower middle fornix, and lower nasal palpebral regions. Conjunctival hydration has been identified as a key external factor influencing glycoconjugate levels, with studies showing a direct correlation: Ralph [61] reported significantly lower glycoconjugate counts in patients with dry keratitis than in healthy individuals. These findings [44,61] underscore the importance of tear fluid hydration for maintaining conjunctival goblet cell health. Accordingly, morphoanatomical studies such as ours are essential for advancing clinical understanding and improving ocular treatments.

Taken together, these histological findings reveal possible differences between dogs and wolves with biological, physiological, evolutionary, and veterinary implications. However, these differences could be partly influenced by postmortem factors, such as the longer

postmortem interval in wolves. In dogs, the thicker epithelium of the bulbar and palpebral conjunctiva, combined with greater PAS and Alcian Blue positive secretion, may suggest better ocular protection and lubrication capabilities, adapted to domestic environments. The more developed tarsal lumen in dogs further supports this hypothesis, allowing for greater storage and steady release of lubricating substances to maintain ocular surface health, particularly in settings with various irritants and pollutants. Conversely, wolves, with their additional aggregates of glandular tissue, may have more concentrated and specific secretions suited to their natural environment, in which the conditions may necessitate different ocular protection mechanisms. The predominance of acidic mucopolysaccharides in the palpebral conjunctiva and fornix of wolves, as opposed to the neutral mucopolysaccharides in dogs, underscores divergent environmental pressures and ocular protection strategies.

The identified histological differences are fundamental for the development of specific veterinary treatments and for improving the clinical management of ocular conditions in dogs and wolves. Furthermore, these findings provide a solid foundation for future research on ocular adaptations in canids and are valuable for conservation and species management programs, highlighting the unique environmental and lifestyle adaptations of each species. In addition to anatomical characterization, this study has broader applications in human medicine. Due to their anatomical similarities with humans, dogs serve as excellent models for studying the surface eye diseases such as keratoconjunctivitis sicca (KCS) [33] and the conjunctival mucosal system [44]. Furthermore, dogs represent the species most commonly affected by spontaneous ocular diseases observed in veterinary practice, serving as relevant models for various human ophthalmic pathologies.

A key limitation of this study is the small sample size for both species. Owing to the protected status and elusive nature of wild animals, access to biologically and demographically comparable samples is extremely restricted. Similarly, in domestic dogs, obtaining naturally deceased individuals of known breed, age, and sex—along with owner consent for scientific use—poses ethical and logistical challenges. The use of dogs of diverse breeds with potential differences in predisposition to specific pathologies represents another potential limitation of this study. However, no anatomical differences were observed among the individuals examined, regardless of their breed-related characteristics. These findings suggest that the features described are consistent across our canine samples. Nevertheless, these findings should be regarded as preliminary, given the limited number of individuals of each species examined.

Although our observations indicate appreciable histological differences between dogs and wolves, we acknowledge the limitations inherent in a qualitative approach. A rigorous morphometric analysis—including measurements of corneal and scleral thickness, conjunctival layers, and glandular areas—would provide quantitative support for these findings. However, such an analysis requires a larger and more homogeneous sample set, ideally comprising individuals of similar age, size, and physiological status. This is particularly difficult to achieve in the case of wolves, where sample availability is extremely limited. Moreover, reliable morphometric comparisons require serial histological sectioning using consistent anatomical landmarks, which is technically challenging given the size and heterogeneity of the samples. Despite these constraints, qualitative anatomical comparisons remain valuable when consistent features are observed across multiple individuals, as is the case in our study. For each structure analyzed, we deliberately selected the most representative areas, and the trends observed were consistently found in all three specimens per species. Thus, the present work represents a qualitative and descriptive approach rather than a quantitative or morphometric analysis. While some of the interspecies differences observed may suggest structural or functional divergence, these observations must be interpreted cautiously, within the context of a limited and heterogeneous sample. This

constraint is common in anatomical studies involving wildlife and does not diminish the value of reporting observable histological and lectin-binding patterns, which may serve as a foundation for future research under more controlled conditions. We acknowledge these limitations and emphasize that the comparative insights provided here are preliminary and should be validated by further studies with larger and more standardized cohorts.

In conclusion, our study presents a descriptive account of the differences in tissue organization, microscopic structure, and glycoconjugate expression patterns in the eye and ocular adnexa between dogs and wolves. While no inferential claims can be drawn due to the descriptive and nonquantitative nature of this research, the observed patterns may serve as a valuable basis for future investigations. A better understanding of species-specific anatomical traits could eventually contribute to refined approaches in both clinical and conservation contexts.

Author Contributions: Conceptualization, A.D.L., M.V.T., P.S.-Q. and I.O.-L.; methodology, M.V.T., F.M.G., S.A.F.A., P.S.-Q. and I.O.-L.; investigation, A.D.L., M.V.T., F.M.G., S.A.F.A., A.L.-B., L.F., P.S.-Q. and I.O.-L.; resources, A.L.-B., L.F. and P.S.-Q.; writing—original draft preparation, F.M.G. and P.S.-Q.; writing—review and editing, A.D.L., P.S.-Q. and I.O.-L.; supervision, P.S.-Q. and I.O.-L.; project administration, P.S.-Q.; funding acquisition, P.S.-Q. All authors have read and agreed to the published version of the manuscript.

Funding: This research was funded by Consello Social da Universidade de Santiago de Compostela, grant number 2022-PU004.

Institutional Review Board Statement: The Authors declare under their own responsibility that, for the present study, ethical review and approval were waived by the Institutional Review Board, as all animals used in the study died due to natural causes or fatal accidents, with no intervention to induce their death for experimental purposes. Specifically, the eyeballs and their adnexa used in this study were collected from three adult dogs sourced from the Rof Codina University Veterinary Hospital at the Faculty of Veterinary Sciences of Lugo. These dogs had died due to various clinical conditions unrelated to the study. Additionally, eyeballs were obtained from three adult wolves originating from wildlife rehabilitation centers located in the provinces of Galicia, which had died due to fatal accidents. The procurement of samples was conducted in strict compliance with the necessary authorizations from the Galician Environment, Territory, and Housing Department, under approval codes EB-009/2020 and EB-007/2021. Therefore, no further ethical review was required, as no experimental procedures were performed on living animals, and all samples were obtained post-mortem from animals that died due to causes independent of the study.

Informed Consent Statement: Not applicable, as this research did not involve any humans.

Data Availability Statement: No new data were created.

Acknowledgments: The authors wish to thank the wildlife recovery centers in Galicia and Dirección Xeral de Patrimonio Natural (Consellería de Medio Ambiente e Ordenación do Territorio, Xunta de Galicia) for authorizing and facilitating the sampling of the animals.

Conflicts of Interest: The authors declare no conflicts of interest.

References

1. Ansari, M.W.; Nadeem, A. Anatomy of the Eyelids. In *Atlas of Ocular Anatomy*; Ansari, M.W., Nadeem, A., Eds.; Springer International Publishing: Cham, Switzerland, 2016; pp. 53–63, ISBN 978-3-319-42781-2.
2. Fine, B.S.; Yanoff, M. *Ocular Histology: A Text and Atlas*, 2nd ed.; Medical Dept., Harper & Row: Hagerstown, MD, USA, 1979.
3. Crespo-Moral, M.; García-Posadas, L.; López-García, A.; Diebold, Y. Histological and Immunohistochemical Characterization of the Porcine Ocular Surface. *PLoS ONE* **2020**, *15*, e0227732. [CrossRef] [PubMed]
4. Gipson, I.K.; Argüeso, P. Role of Mucins in the Function of the Corneal and Conjunctival Epithelia. *Int. Rev. Cytol.* **2003**, *231*, 1–49. [CrossRef] [PubMed]
5. Watanabe, H. Significance of Mucin on the Ocular Surface. *Cornea* **2002**, *21*, S17–S22. [CrossRef] [PubMed]

6. Knop, E.; Knop, N. The Role of Eye-associated Lymphoid Tissue in Corneal Immune Protection. *J. Anat.* **2005**, *206*, 271–285. [CrossRef]
7. García-Posadas, L.; Contreras-Ruiz, L.; Soriano-Romaní, L.; Dartt, D.A.; Diebold, Y. Conjunctival Goblet Cell Function: Effect of Contact Lens Wear and Cytokines. *Eye Contact Lens Sci. Clin. Pract.* **2016**, *42*, 83–90. [CrossRef]
8. Sandøe, P.; Palmer, C.; Corr, S.; Serpell, J. *History of Companion Animals and the Companion Animal Sector*; John Wiley and Sons: Hoboken, NJ, USA, 2015; pp. 8–23.
9. Smythe, R.H. The Eye of the Dog. In *Vision in the Animal World*; Palgrave Macmillan: London, UK, 1975; pp. 60–74, ISBN 978-1-349-02535-0.
10. Pedraza Aguirre, G.; Beltrán Bareño, A.A. Queratoconjuntivitis Seca Y Cataratas: Algunas Afecciones Oftálmicas Comunes en Caninos. 2019. Available online: https://repository.ucc.edu.co/entities/publication/9631476c-7533-4016-9ed7-5d6c18ba6713 (accessed on 15 April 2025).
11. Cabral, V.P.; Laus, J.L.; Dagli, M.L.Z.; Pereira, G.T.; Talieri, I.C.; Monteiro, E.R.; Mamede, F.V. Canine Lacrimal and Third Eyelid Superficial Glands' Macroscopic and Morphometric Characteristics. *Cienc. Rural* **2005**, *35*, 391–397. [CrossRef]
12. Lantyer-Araujo, N.L.; Silva, D.N.; Estrela-Lima, A.; Muramoto, C.; Libório, F.d.A.; da Silva, É.A.; Oriá, A.P. Anatomical, Histological and Computed Tomography Comparisons of the Eye and Adnexa of Crab-Eating Fox (*Cerdocyon thous*) to Domestic Dogs. *PLoS ONE* **2019**, *14*, e0224245. [CrossRef]
13. Mowat, F.M.; Peichl, L. Ophthalmology of Canidae: Foxes, Wolves, and Relatives. In *Wild and Exotic Animal Ophthalmology*; Montiani-Ferreira, F., Moore, B.A., Ben-Shlomo, G., Eds.; Springer International Publishing: Cham, Switherland, 2022; pp. 181–214, ISBN 978-3-030-81272-0.
14. Harwell, G.M.; Angell, J.A.; Merideth, R.E.; Carley, C. Chronic Superficial Keratitis in a Mexican Wolf. *J. Am. Vet. Med. Assoc.* **1985**, *187*, 1268. [CrossRef]
15. Acton, A.E.; Beale, A.B.; Gilger, B.C.; Stoskopf, M.K. Sustained Release Cyclosporine Therapy for Bilateral Keratoconjunctivitis Sicca in a Red Wolf (*Canis rufus*). *J. Zoo Wildl. Med.* **2006**, *37*, 562–564. [CrossRef]
16. Watsky, M.A.; Jablonski, M.M.; Edelhauser, H.F. Comparison of Conjunctival and Corneal Surface Areas in Rabbit and Human. *Curr. Eye Res.* **1988**, *7*, 483–486. [CrossRef]
17. Loiseau, A.; Raîche-Marcoux, G.; Maranda, C.; Bertrand, N.; Boisselier, E. Animal Models in Eye Research: Focus on Corneal Pathologies. *Int. J. Mol. Sci.* **2023**, *24*, 16661. [CrossRef] [PubMed]
18. Pei, W.; Chen, J.; Wu, W.; Wei, W.; Yu, Y.; Feng, Y. Comparison of the Rabbit and Human Corneal Endothelial Proteomes Regarding Proliferative Capacity. *Exp. Eye Res.* **2021**, *209*, 108629. [CrossRef]
19. Sebbag, L.; Mochel, J.P. An Eye on the Dog as the Scientist's Best Friend for Translational Research in Ophthalmology: Focus on the Ocular Surface. *Med. Res. Rev.* **2020**, *40*, 2566–2604. [CrossRef]
20. Schrader, S.; Mircheff, A.K.; Geerling, G. Animal Models of Dry Eye. In *Developments in Ophthalmology*; Geerling, G., Brewitt, H., Eds.; KARGER: Basel, Switherland, 2008; Volume 41, pp. 298–312, ISBN 978-3-8055-8376-3.
21. Mäkeläinen, S.; Gòdia, M.; Hellsand, M.; Viluma, A.; Hahn, D.; Makdoumi, K.; Zeiss, C.J.; Mellersh, C.; Ricketts, S.L.; Narfström, K.; et al. An ABCA4 Loss-of-Function Mutation Causes a Canine Form of Stargardt Disease. *PLoS Genet.* **2019**, *15*, e1007873. [CrossRef]
22. Dufour, V.L.; Aguirre, G.D. Canine Models of Inherited Retinal Diseases: From Neglect to Well-Recognized Translational Value. *Mamm. Genome* **2025**, *36*, 500–510. [CrossRef] [PubMed]
23. Ortiz-Leal, I.; Torres, M.V.; Villamayor, P.R.; Fidalgo, L.E.; López-Beceiro, A.; Sanchez-Quinteiro, P. Can Domestication Shape Canidae Brain Morphology? The Accessory Olfactory Bulb of the Red Fox as a Case in Point. *Ann. Anat.* **2022**, *240*, 151881. [CrossRef] [PubMed]
24. Bera, G.; Das, R.N.; Roy, P.; Ghosh, R.; Islam, N.; Mishra, P.K.; Chatterjee, U. Utility of PAS and β-Catenin Staining in Histological Categorisation and Prediction of Prognosis of Hepatoblastomas. *Pediatr. Surg. Int.* **2017**, *33*, 961–970. [CrossRef] [PubMed]
25. Torres, M.V.; Ortiz-Leal, I.; Villamayor, P.R.; Ferreiro, A.; Rois, J.L.; Sanchez-Quinteiro, P. The Vomeronasal System of the Newborn Capybara: A Morphological and Immunohistochemical Study. *Sci. Rep.* **2020**, *10*, 13304. [CrossRef]
26. Sanmartín-Vázquez, E.; Ortiz-Leal, I.; Torres, M.V.; Kalak, P.; Kubiak-Nowak, D.; Dzięcioł, M.; Sanchez-Quinteiro, P. Functional Role of the Incisive Duct in Neonatal Dogs. *Cells Tissues Organs* **2025**, *214*, 167–184. [CrossRef]
27. Salazar, I.; Lombardero, M.; Cifuentes, J.M.; Quinteiro, P.S.; Aleman, N. Morphogenesis and Growth of the Soft Tissue and Cartilage of the Vomeronasal Organ in Pigs. *J. Anat.* **2003**, *202*, 503–514. [CrossRef]
28. Plendl, J.; Sinowatz, F. Glycobiology of the Olfactory System. *Cells Tissues Organs* **1998**, *161*, 234–253. [CrossRef] [PubMed]
29. Devi, R.V.; Basil-Rose, M.R. Lectins as Ligands for Directing Nanostructured Systems. *CDD* **2018**, *15*, 448–452. [CrossRef] [PubMed]
30. Ortiz-Leal, I.; Torres, M.V.; López-Callejo, L.N.; Fidalgo, L.E.; López-Beceiro, A.; Sanchez-Quinteiro, P. Comparative Neuroanatomical Study of the Main Olfactory Bulb in Domestic and Wild Canids: Dog, Wolf and Red Fox. *Animals* **2022**, *12*, 1079. [CrossRef] [PubMed]

31. Ortiz-Leal, I.; Torres, M.V.; Barreiro-Vázquez, J.; López-Beceiro, A.; Fidalgo, L.; Shin, T.; Sanchez-Quinteiro, P. The Vomeronasal System of the Wolf (*Canis lupus signatus*): The Singularities of a Wild Canid. *J. Anat.* **2024**, *245*, joa.14024. [CrossRef]
32. Ortiz-Leal, I.; Torres, M.V.; Vargas-Barroso, V.; Fidalgo, L.E.; López-Beceiro, A.M.; Larriva-Sahd, J.A.; Sánchez-Quinteiro, P. The Olfactory Limbus of the Red Fox (*Vulpes vulpes*). New Insights Regarding a Noncanonical Olfactory Bulb Pathway. *Front. Neuroanat.* **2023**, *16*, 1097467. [CrossRef]
33. Strom, A.R.; Cortés, D.E.; Rasmussen, C.A.; Thomasy, S.M.; McIntyre, K.; Lee, S.; Kass, P.H.; Mannis, M.J.; Murphy, C.J. In Vivo Evaluation of the Cornea and Conjunctiva of the Normal Laboratory Beagle Using Time- and Fourier-domain Optical Coherence Tomography and Ultrasound Pachymetry. *Vet. Ophthalmol.* **2016**, *19*, 50–56. [CrossRef]
34. *Wild and Exotic Animal Ophthalmology: Volume 2: Mammals*; Montiani-Ferreira, F., Moore, B.A., Ben-Shlomo, G., Eds.; Springer International Publishing: Cham, Switzerland, 2022; ISBN 978-3-030-81272-0.
35. IUCN Canis Lupus; Boitani, L.; Phillips, M.; Jhala, Y. The IUCN Red List of Threatened Species 2023: E.T3746A247624660 2018. Available online: https://www.iucnredlist.org/species/23062/193903628 (accessed on 15 April 2025).
36. Cerrada, I.; Leiva, M.; Vilao, R.; Peña, T.; Ríos, J. Follicular Conjunctivitis in Dogs: A Retrospective Study (2007–2022). *Vet. Ophthalmol.* **2024**, *27*, 310–317. [CrossRef]
37. Ollivier, F.J. Bacterial Corneal Diseases in Dogs and Cats. *Clin. Tech. Small Anim. Pract.* **2003**, *18*, 193–198. [CrossRef]
38. Startup, F.G. Corneal Ulceration in the Dog. *J. Small Anim. Pract.* **1984**, *25*, 737–752. [CrossRef]
39. Peña, M.T.; Leiva, M. Canine Conjunctivitis and Blepharitis. *Vet. Clin. N. Am. Small Anim. Pract.* **2008**, *38*, 233–249. [CrossRef]
40. El-naseery, N.; El-behery, E.; El-Ghazali, H.; El-Hady, E. The Structural Characterization of the Lacrimal Gland in the Adult Dog (*Canis familiaris*). *Benha Vet. Med. J.* **2016**, *31*, 106–116. [CrossRef]
41. Zwingenberger, A.L.; Park, S.A.; Murphy, C.J. Computed Tomographic Imaging Characteristics of the Normal Canine Lacrimal Glands. *BMC Vet. Res.* **2014**, *10*, 116. [CrossRef] [PubMed]
42. Williams, D.L.; Tighe, A. Immunohistochemical Evaluation of Lymphocyte Populations in the Nictitans Glands of Normal Dogs and Dogs with Keratoconjunctivitis Sicca. *Open Vet. J.* **2018**, *8*, 47. [CrossRef]
43. Araújo, R.L.S.; Corrêa, J.R.; Galera, P.D. Ultrastructural Morphology of Goblet Cells of the Conjunctiva of Dogs. *Vet. Ophthalmol.* **2019**, *22*, 891–897. [CrossRef]
44. Moore, C.P.; Wilsman, N.J.; Nordheim, E.V.; Majors, L.J.; Collier, L.L. Density and Distribution of Canine Conjunctival Goblet Cells. *Investig. Ophthalmol. Vis. Sci.* **1987**, *28*, 1925–1932.
45. Umeda, Y.; Nakamura, S.; Fujiki, K.; Toshida, H.; Saito, A.; Murakami, A. Distribution of Goblet Cells and MUC5AC mRNA in the Canine Nictitating Membrane. *Exp. Eye Res.* **2010**, *91*, 721–726. [CrossRef]
46. Murphy, C.; Samuelson, D.A.; Pollock, R.V.H. The Eye. In *Miller's Anatomy of the Dog*; Elsevier: Amsterdam, The Netherlands, 2012; pp. 746–785. Available online: https://www.researchgate.net/publication/280090396_C_J_Murphy_DA_Samuelson_RVH_Pollock_Ch_21_The_Eye_Miller's_Anatomy_of_the_Dog_2012_746-785 (accessed on 15 April 2025).
47. Paszta, W.; Klećkowska-Nawrot, J.E.; Goździewska-Harłajczuk, K. Anatomical and Morphometric Evaluation of the Orbit, Eye Tunics, Eyelids and Orbital Glands of the Captive Females of the South African Painted Dog (*Lycaon pictus pictus* Temminck, 1820) (Caniformia: Canidae). *PLoS ONE* **2021**, *16*, e0249368. [CrossRef]
48. Hartstone-Rose, A.; Werdelin, L.; De Ruiter, D.J.; Berger, L.R.; Churchill, S.E. The Plio-Pleistocene Ancestor of Wild Dogs, *Lycaon sekowei* n. *Sp. J. Paleontol.* **2010**, *84*, 299–308. [CrossRef]
49. Gasser, K.; Fuchs-Baumgartinger, A.; Tichy, A.; Nell, B. Investigations on the Conjunctival Goblet Cells and on the Characteristics of Glands Associated with the Eye in the Guinea Pig. *Vet. Ophthalmol.* **2011**, *14*, 26–40. [CrossRef]
50. Peichl, L. Catecholaminergic Amacrine Cells in the Dog and Wolf Retina. *Vis. Neurosci.* **1991**, *7*, 575–587. [CrossRef]
51. Peichl, L. Morphological Types of Ganglion Cells in the Dog and Wolf Retina. *J. Comp. Neurol.* **1992**, *324*, 590–602. [CrossRef]
52. Peichl, L. Topography of Ganglion Cells in the Dog and Wolf Retina. *J. Comp. Neurol.* **1992**, *324*, 603–620. [CrossRef] [PubMed]
53. Caeiro, C.; Guo, K.; Mills, D. Dogs and Humans Respond to Emotionally Competent Stimuli by Producing Different Facial Actions. *Sci. Rep.* **2017**, *7*, 15525. [CrossRef] [PubMed]
54. Smith, H.F.; Felix, M.A.; Rocco, F.A.; Lynch, L.M.; Valdez, D. Adaptations to Sociality in the Mimetic and Auricular Musculature of the African Wild Dog (*Lycaon pictus*). *Anat. Rec.* **2024**, *307*, 3327–3343. [CrossRef]
55. Ruiz-Rubio, S.; Ortiz-Leal, I.; Torres, M.V.; Elsayed, M.G.A.; Somoano, A.; Sanchez-Quinteiro, P. The Accessory Olfactory Bulb in Arvicola Scherman: A Neuroanatomical Study in a Subterranean Mammal. *Animals* **2024**, *14*, 3285. [CrossRef] [PubMed]
56. Torres, M.V.; Ortiz-Leal, I.; Sanchez-Quinteiro, P. Pheromone Sensing in Mammals: A Review of the Vomeronasal System. *Anatomia* **2023**, *2*, 346–413. [CrossRef]
57. Salazar, I.; Sánchez Quinteiro, P. Differential Development of Binding Sites for Four Lectins in the Vomeronasal System of Juvenile Mouse: From the Sensory Transduction Site to the First Relay Stage. *Brain Res.* **2003**, *979*, 15–26. [CrossRef]
58. Tuori, A.; Virtanen, I.; Uusitalo, H. Lectin Binding in the Anterior Segment of the Bovine Eye. *Histochem. J.* **1994**, *26*, 787–798. [CrossRef]

59. Qaddoumi, M.; Lee, V.H.L. Lectins as Endocytic Ligands: An Assessment of Lectin Binding and Uptake to Rabbit Conjunctival Epithelial Cells. *Pharm. Res.* **2004**, *21*, 1160–1166. [CrossRef]
60. Rittig, M.; Brigel, C.; Lutjen-Drecoll, E. Lectin-Binding Sites in the Anterior Segment of the Human Eye. *Graefe's Arch. Clin. Exp. Ophthalmol.* **1990**, *228*, 528–532. [CrossRef]
61. Ralph, R.A. Conjunctival Goblet Cell Density in Normal Subjects and in Dry Eye Syndromes. *Investig. Ophthalmol.* **1975**, *14*, 299–302.